Fall 12-18-2017

Objective Measures of Electrophysiological Responses of Children with Idiopathic Autism Spectrum Disorder and Phelan-McDermid Syndrome to a Contrast-Reversing Checkerboard

Chloe Brittenham
CUNY Hunter College

Objective Measures of Electrophysiological Responses of Children with Idiopathic Autism Spectrum Disorder and Phelan-McDermid Syndrome to a Contrast-Reversing Checkerboard

by

Chloe Brittenham

Submitted in partial fulfillment
of the requirements for the degree of
Master of Arts of Psychology, Hunter College
The City University of New York

2017

	Thesis Sponsor:
December 18, 2017	Dr. James Gordon
Date	Signature
December 18, 2017	Dr. Vance Zemon
Date	Signature of Second Reader
December 18, 2017	Dr. Paige Siper
Date	Signature of Third Reader

Abstract

The heterogeneity of autism presents many challenges in understanding the disorder. About one thousand genes are implicated in autism spectrum disorder (ASD) and there is high variability in the excitatory/inhibitory (EI) profiles of these individuals. Studying monogenetic disorders that present with ASD is one way to examine the common neural pathways affected in autism. The current study employs objective measures to examine visual evoked potential (VEP) responses of children with idiopathic autism (iASD) and Phelan-Mcdermid syndrome (PMS) to a contrast-reversing checkerboard in both long (60-second) and short (2-second) duration conditions. Responses are compared with those of typically developing (TD) children. Analyses of the response include multilevel linear modeling, time-domain analyses, and objective frequency domain measures including magnitude squared coherence and a power spectra analysis. This is the first use of this analysis of power spectra to examine the VEPs of children with autism and the first study to compare the ratio of power between two conditions, long- and short-duration in children with iASD and PMS. We argue that this form of analysis be included in evaluations of VEPs as it has the potential to reveal objective biomarkers and is not susceptible to the error associated with subjective-based time-domain analyses. PMS and iASD groups showed decreased amplitudes at P60-N75 and N75-P100 as well less coherence in frequency ranges associated with excitatory activity. PMS and iASD groups showed preserved inhibitory activity as indicated by P100-N135 amplitude and low frequency range activity. iASD and PMS groups showed decreased power in the long condition across frequencies. The TD group showed this effect only in the high frequency range. Implications of these objective measures of analyses are discussed as well as potential attentional and adaptation effects seen between the two conditions.

Objective Measures of Electrophysiological Responses of Children with Idiopathic Autism Spectrum Disorder and Phelan-McDermid syndrome to a Contrast-Reversing Checkerboard

ASD. Autism spectrum disorder (ASD) is a neurodevelopmental disorder characterized by deficits in social communication and repetitive or restricted behaviors or interests (DSM 5). As part of the diagnostic criteria for ASD, symptoms must present in early development and symptoms must have significant adverse effects on occupational and social functioning (DSM 5).

History of autism. The first description of autism was by Dr. Leo Kanner in 1943 and separately by Hans Asperger in 1944. Kanner's descriptions of 11 case studies characterized affected children as socially aloof, with severe language delays or abnormalities, as well as an insistence on sameness. Asperger with his 1944 description of the disorder identified affected children as having intact language skills with social deficits and narrow interests (as cited in Kim & Lord, 2013). ASD has since been consolidated into a single disorder in the DSM-5. Prior to this, Pervasive Developmental Disorder-Not Otherwise Specified (PDD-NOS) and Asperger's syndrome were separate classifications with different criteria from autistic disorder as described in the DSM-IV.

Though the cause of autism is still unknown, several risk factors for ASD have been identified. Studies of identical twins and siblings have demonstrated the heredity of the disorder. Identifiable chromosomal conditions as well as intellectual disability (ID) and psychiatric disorders present in some individuals with autism (Kim & Lord, 2013). The concordance ratio when comparing monozygotic and dizygotic twins is 10 to 1. This finding as well as the rate of ASD diagnoses and/or symptoms within families who have an individual diagnosed with autism provides a strong argument for a genetic etiology (Betancur, 2011).

However, family studies have also revealed that "transmission" of ASD is complex. Buxbaum (2009) reviews evidence for the etiology model of multiple rare variants. The multiple rare variant model may explain the heterogenic nature of ASD. Analyses of genetic profiles of individuals with ASD have highlighted the role of genetics in the likelihood of the disorder. ASD has in some cases been linked to mutations across a great number of genes and several studies have identified numerous risk genes (Betancur, 2011). ASD seems to be the result of multiple rare genetic variants, in particular those that implicate synaptic genes and neuronal genes that govern common molecular pathways. Of interest to the current study are mutations and deletions in the *SHANK3* gene, on chromosome 22q13.3, resulting in Phelan Mc-Dermid syndrome (PMS) (Buxbaum, 2009).

Prevalence. Prevalence rates of ASD have risen drastically over the past decade. As of 2014, The Centers for Disease Control and Prevention's Autism and Developmental Disabilities Monitoring (ADDM) Network estimate the prevalence rate to be about 1 in 68 (Christensen et al., 2016). The disorder continues to be more prevalent in males than females (1 in 42 males and 1 in 189 females) (Christensen, et al., 2016). In a study of 49 prevalence surveys from 1966 to 2011 across 21 different countries, the most accurate estimate at that time of publication (French, Bertone, Hyde, & Fombonne, 2013) was 26/10,000. It is unclear whether this increase in prevalence is due to a greater incidence of the disorder or to improved diagnostic criteria, diagnostic approach, improved access to services, and overall increased awareness of the disorder.

Etiological heterogeneity. In a 2011 review, Betancur highlights the progress that has been made in identifying genomic loci (44) and disease genes (103) implicated in ASD. Betancur

stresses that from what we now know about the "rare nature of these variants" autism is best understood as the behavioral manifestation of many genomic and genetic disorders.

While these findings have aided in our understanding of the etiology of the disorder, the broad range of risk genes involved in cases of autism as well as the diverse spectrum of symptom expression has presented many challenges in the treatment of ASD.

Phelan-McDermid Syndrome. Phelan-McDermid syndrome, also known as 22q13 deletion syndrome, is a single-gene cause of ASD characterized by the loss of one functional copy of the *SHANK3* gene which is located at the terminal of chromosome 22. Loss of one functional copy is referred to as haploinsufficiency. Phelan-McDermid syndrome is responsible for about 0.5% of incidences of autism. *SHANK3* functions to encode a protein responsible for the scaffolding of postsynaptic density of glutamatergic synapses which ultimately affects synaptic function (Harony, H., Günal, O. & Buxbaum, J., 2013).

Studies of the shortest microdeletions, have allowed the identification of a "critical region" where three genes, *ACR, RABL2B,* and *SHANK3* reside. *SHANK3* has been identified as the most likely contributor to the neurobehavioral deficits in Phelan-McDermid syndrome. Microdeletions affecting only *SHANK3* still result in ASD symptoms (Harony, Günal, & Buxbaum, 2013).

Behavioral heterogeneity. Genetic causes can be identified in approximately 20% of cases, however, there remains significant heterogeneity within individuals with ASD for which a genetic cause remains unknown (referred to as idiopathic ASD or iASD). Heterogeneity of behavior in autism has even been described in identical twins (Kim & Lord, 2013). Manifestations of autistic behavior vary widely in level of intellectual impairment, verbal and

nonverbal communication, severity of repetitive and restricted behaviors, and sensory-reactivity (Georgiades et al., 2013). It is also thought that these different symptom presentations may require different types of interventions to produce meaningful improvement in behavior.

The defining characteristics of Phelan-McDermid syndrome include global developmental delay, absent or delayed speech, mild dysmorphic features, ASD, intellectual disability (ID), and global developmental delay (Soorya et al., 2013).

Electrophysiological heterogeneity. Electrophysiological studies of forms of ASD with known causes such as PMS can provide information about the underlying biology of autism spectrum disorder. Several single-gene causes of ASD, such as PMS, converge on the same "molecular pathways" responsible for the function and support of synaptic transmission (Costales & Kolevzon, 2015). Treatment methods developed specifically for PMS may also prove effective for other forms of ASD, including for individuals without a known genetic cause who show similar neural profiles.

Harony-Nicolas, De Rubeis, Kolevzon, and Buxbaum (2015) stress the importance of the use of animal models to identify effective treatments for Phelan-McDermid syndrome. Current behavioral treatments for PMS and ASD broadly often include applied behavior analysis (ABA), speech therapy, occupational therapy, and physical therapy. Medications may be used to address comorbid symptoms such as anxiety and hyperactivity. However, to date there are no treatments for "core deficits at the molecular, cellular or circuitry level" (Harony-Nicolas, De Rubeis, Kolevzon, & Buxbaum, 2015, p.1866).

While the neurological basis for the characterizing symptoms of ASD are still not well understood, weaker electrophysiological responses measured through techniques such as visual evoked potentials (VEPs) reflect an altered excitation/inhibition (E/I) profile (Siper et al., 2016).

Rubenstein and Merzenich introduced the hypothesis of an altered E/I profile in 2003. Rubenstein and Merzenich posit increased ratio of excitation to inhibition. This idea is based on experimental evidence of altered GABAergic and glutamatergic functioning basic studies of the disorder. About 30% of individuals with autism have seizures and 70% have spike activity present in EEG recordings (Blatt, 2013) This, along with the finding of decreased density of GABA-A receptors in postmortem tissue of ASD individuals (Blatt et al. 2001) has led some researchers to posit that excitatory circuitry may be advantaged and GABA is suppressed (Hussman, 2001). The concept that there is some abnormality in GABA and also higher tonic excitation in ASD has led to the hypothesis of an increased ratio of excitation to inhibition in autism (Blatt, 2013).

Animal models have provided some evidence both in support of this hypothesis and contradictory, or complicating to it as well. Animal models of ASD have presented evidence for enhanced glutamatergic activity in syndromes such as Fragile X syndrome, while mouse models of PMS show the opposite effect on excitatory activity. The excitatory/inhibitory profiles of ASD are thus highly variable and studying single-gene causes of ASD allows us to better understand differences in E/I balance based on underlying neurobiological mechanisms. Being able to group individuals based on their excitatory and inhibitory activity would be a useful tool for individualized focused treatment that can directly confront the problem of heterogeneity in autism (Siper et al., 2016).

Visual evoked potential (VEP). Visual evoked potentials have long been used to aid in the diagnosis and understanding of several neurological disorders including ASD. Visual evoked potential, or VEP, refers to the electrical response evoked by simple visual stimuli recorded from the area of the scalp over the visual cortex. Waveforms of the VEP are extracted from the recording through a process of signal averaging. Signal averaging is facilitated by linking the onset of the stimulus to a trigger pulse. In signal averaging, the relevant epochs (following the stimulus presentation) are repeated and then added together. This results in the averaging-away of random EEG activity that is not evoked by the stimulus presentation. VEPs are widely used to assess the functional integrity of visual pathways. VEPs were first used in clinical encephalography during the 1930s (Creel, 2012).

VEPs are typically recorded from the midline of the occipital scalp, which covers the calcarine fissure; this location is identified by the 10-20 International system for electrode placement at Oz. The current study records a single channel from Oz (where the response to the stimuli is largest) referenced to a site on the vertex of the head, Cz (Creel, 2012).

One of the most widely used stimuli in visual evoked potential recording is the contrast-reversing checkerboard. This is an image of black and white checks which reverse typically every 500 ms. This type of pattern reversal is common and it has high inter-subject reliability. Contrast-reversing checkerboard stimuli reliably produce several distinct deflections in the response: P60, N75, P100, N135, P200, and N250. P60 is a positive peak at 60 ms, reflecting activation of the primary visual cortex (PVC) by afferents from the lateral geniculate nucleus. N75 is a negative trough at 75 ms which reflects depolarization and glutamatergic postsynaptic activity radiating to the superficial layers of the PVC (Creel, 2012). P100 is a positive peak at

100 ms reflecting hyperpolarization and GABAergic activity, thought to be generated by the superficial layers of the striate (Zemon, Kaplan, & Ratliff, 1980). N135 is a negative trough at 135 ms which is thought to be associated with attentional mechanisms (selective attention) generated from the parietal lobe, striate and extrastriate areas (Shigeto et al., 1998; Di Russo et al., 2002).

Previous electrophysiological research of ASD has shown increased noise and smaller amplitudes across early deflections of the response. A 2016 study by Siper et al. showed that a new shortened version of a commonly employed VEP stimulus (contrast-reversing checkerboard, 2 seconds, 10 trials) gave reliable findings, comparable to the well-utilized 60-second version. Through using these shortened trials, individuals of varying levels of functioning are able to participate in VEP studies. Sensory abnormalities and attentional deficits may often interfere with individuals' ability to fixate for a full 60 seconds.

The purpose of the present study is to quantify differences between idiopathic ASD and a subtype of ASD, Phelan-McDermid syndrome, using electrophysiological techniques. We expect the analysis of the early deflections of the response of children with idiopathic ASD to replicate previous research by Siper et al (2016). Results from that study indicate that children with ASD have significantly smaller amplitudes than typically developing (TD) children in response to contrast-reversing checkerboards, particularly in the earlier components of the VEP, P60-N75 and N75-P100. These results are consistent with previous studies that have suggested attenuated activity in the cortex for individuals with ASD. P60-N75 amplitude indicates weakened excitatory input to the cortex, which in turn results in reduced inhibition as shown by the reduced N75-P100 amplitude. The proportional loss of excitation to inhibition suggests that there is no

significant deficit to intracortical inhibition. These findings suggest a deficit in the initial excitatory input to the cortex, rather than a marked deficit in inhibition throughout the cortex (Siper et al, 2016). The results of this study dispute Rubenstein and Merzenich's (2003) theory of an altered E/I profile in which there is higher tonic excitation and impaired inhibition in ASD. Siper et al. suggest that disorder may be more accurately characterized by a deficit in excitation rather than inhibition. Furthermore, Siper et al. (2016) found that latency did not differ between groups, which suggests that there is no delay in the transmission of information to the cortex.

Results from the frequency domain reveal a marked reduction of high frequency activity in the ASD groups, which suggests a loss of excitatory cortical input. Potential alterations in the frequency domain will also be important to compare with the PMS group. Siper et al. also found greater variability in both low (Band 3, 30 - 36 Hz) and high frequency gamma-wave activity (Band 4, 38-48 Hz) bands in ASD groups. This finding supports abnormal gamma-wave activity in ASD and has been implicated in the functioning of GABA-ergic interneurons (Siper et al, 2016).

Justification. The current study utilized a transient VEP to a contrast-reversing checkerboard stimulus and a new ratio statistic to compare results of long- and short-duration conditions. These measures were taken in an effort to locate potential biomarkers relevant to idiopathic ASD and a genetically-defined disorder which presents with ASD (PMS) using traditionally measured components of the VEP, as well as to clarify differences and similarities between and within these groups. The present study also includes a preliminary examination of later deflections of the VEP, N135, P200, and N250, which are not commonly included in VEP analyses. P100-N135 is of particular interest as it has been found to reflect early attentional mechanisms. The

careful study of early attentional mechanisms is important in understanding the later cognitive and behavioral impairments present in ASD, particularly because sensory and attentional abnormalities commonly present with ASD and may impact higher-level cognitive processes. This study will also add to the knowledge of late components of the VEP, which have rarely been included in analyses.

This study can provide further information about the ways in which ASD affects the brain. This kind of insight can help determine more personalized therapeutic interventions. Changes in the VEP can also be measured to assess the response to intervention.

Additionally, the current study employs an analysis of power spectra, which has never before been utilized in this way to examine individuals with ASD. This is the first study to not only inspect and compare power of frequency bands in autism but also to compare the ratio of power between two conditions, long- and short-duration. The current paper argues that this form of analysis should be included in clinical evaluations of VEPs as it is capable of revealing objective biomarkers given that it is not vulnerable to the same margin of error associated with subjective-based time-domain analyses.

Method

Participants

Fifty-five children between the ages of one and 18 years participated in the present study. Data was collected at the Seaver Autism Center for Research and Treatment and provided by Dr. Siper's lab for this project. Data from two participants were removed due to missing standard runs. The sample analyzed included data from 53 children (M_{age} = 8.23 years, SD = 3.69), 12 TD participants, 7 males and 5 females (M_{age} = 8.05 years, SD = 2.31), 24 participants with iASD, 21

males and 3 females, (M_{age} = 8.27 years, SD = 3.32), and 17 participants with PMS, 8 males and 9 females (M_{age} = 8.28 years, SD = 4.98). Overall there was no significant difference in age between the TD, iASD, or PMS groups, $F(2, 50) = .017$, $p = .984$.

Participants with ASD met diagnostic criteria based on the Diagnostic and Statistical Manual of Mental Disorders, Fifth Edition (DSM-5), were evaluated using standard assessments which included the Autism Diagnostic Interview-Revised (ADI-R) and the Autism Diagnostic Observation Schedule, Second Edition (ADOS-2, Lord et al., 2012). The Seaver Autism Center also provided genetic testing for participants in the iASD and PMS groups. Children were included in the iASD group only if no genetic abnormalities were found. Phelan-McDermid syndrome was verified using chromosomal microarray analysis as well as targeted sequencing.

Apparatus

Stimuli were presented and recorded with the use of a Neucodia system (VeriSci Corp., USA). The Neucodia system provides automatic artifact detection, in which EEG recordings affected by drift/saturation or extreme 60-Hz noise were rejected. For the short condition (2 s, ten trials) the EEG epoch was automatically deleted if an artifact was identified. If an artifact was detected in the standard run (60s, one trial) the entire run was rejected and repeated. The EEG signal was amplified and digitized (gain = 20,000); the bandpass filter was set for 0.5-100 Hz.

Stimuli

The stimulus consisted of a black and white checkerboard pattern of 32 x 32 checks. Check size was 18.75 minarc. The stimulus field subtended 10 degrees x 10 degrees of visual angle. The average luminance of the display was ~50 cd/m^2. The stimulus was contrast-reversed

with a 1 Hz square-wave modulation at 100 percent contrast. The stimulus was presented in two versions: the first, standard 60-second stimulation, and the second, a short condition during which the stimulus was presented ten three-second trials, each of which consisted of approximately one second of adaptation and two seconds of VEP epoch. The sequence of condition presentation was varied across participants.

Procedure

Prior to the experiment, participants were given a visual schedule which outlined the procedure. Three-gold cup surface electrodes were secured to the midline of the scalp using water-soluble paste. Participants were seated 114 cm from the screen. Electrodes were placed according to the International 10-20 system. An active electrode was at Oz, a reference electrode was placed at Cz, and a ground electrode at Pz, located between the active and reference. The output from these electrodes produced a single electrophysiological channel. Visual evoked potentials were synchronized to the frame rate of the display. Participants were prompted to focus on a fixation cross presented in the center of the screen. The experimenter monitored the participant's gaze through the use of an infrared camera to ensure proper fixation. A research assistant was also present to assist in behavior management.

Analysis

Analysis of the data was completed by two main approaches: through examining the latency and amplitude of the waveforms' peak deflections (time-domain analysis) and by calculating the power and coherence of the frequency bands that contributed to the response (frequency-domain analysis).

Waveforms were frequency analyzed and reconstructed through the application of a discrete Fourier transform, conducted on the VEP responses for each condition, computed by the Neucodia system. Harmonic frequencies were extracted and even harmonics 2-84 Hz, excluding 60 Hz, were used to rebuild the response.

Time-domain analyses. The stimulus in this study (contrast-reversing checkerboard) has been shown to reliably produce certain peaks and troughs within a consistent range of milliseconds following stimulus onset. The first peak typically occurs at approximately 60 ms (P60), followed by a trough at about 75 milliseconds (N75), then a positive peak at approximately 100 ms (P100), a negative peak at about 135 ms (N135), and two less defined points: a peak at about 200 ms (P200) and a final trough at about 250 ms (N250).

Peak-to-trough amplitude and latency were determined first by the Neucodia system which uses a preset window of time for each component and selects the most extreme point (in μV) within that window. If the window was too narrow, too early, or late to accurately detect the peak, the window was widened or shifted until the correct point was selected. Each response was visually inspected and if necessary, the window in Neucodia was changed to meet these criteria.

Amplitude of each component is computed by taking the absolute value of peak-to-trough (or trough to peak) μV for P60-N75, N75-P100, P100-N135, N135-P200, and P200-N250. The apex of the peak occurs at a point in time measured in milliseconds. This is taken as the latency (peak time) of the component for P60, N75, P100, N135, P200, and N250.

Frequency-domain analyses. A discrete Fourier transform was applied to extract sine and cosine coefficients, which were used to compute amplitude and phase values for the even harmonics. Magnitude squared coherence (MSC) is the coherence of a participant's responses

within one condition over several repeated trials. MSC is a statistic developed to assess the integrity and coherence of responses in grouped frequency bands. MSC reveals how much of the measured response can be attributed to the input signal and how much is noise. MSC applied to a band of frequencies is the ratio of the estimate of *signal power* to *signal plus noise* power for that range of frequencies. This statistic ranges from 0 to 1, 0 being no signal present, and 1 meaning that a pure signal is present without noise at the given frequencies. Critical values for each band of frequencies are determined based on the number of harmonics included in that band (Zemon et al., 2009).

In the present study, MSC was employed to examine the coherence of responses in six distinct bands of frequencies across runs. The grouping of particular frequencies into these bands is based on previous work utilizing principal component analysis (PCA) in a 2009 study by Zemon et al. In that study, Zemon et al. obtained the frequencies of each epoch through Fourier analysis and then used MSC to measure the significance of each frequency component. PCA produced six distinct bands of frequency components which were highly correlated with the characteristic deflections of the visual evoked potential. Zemon and Gordon (2017) show that this form of analysis is highly reliable and reproducible for individuals and provides more objective measures of the response as compared to the commonly used time domain analysis. The current study groups frequencies into bands based on and utilizes MSC based on this past work (2009).

The six relevant bands are grouped in the following ways: Band 1, 6 - 10 Hz; Band 2, 12 - 28 Hz; Band 3, 30 - 36 Hz; Band 4, 38-48 Hz; Band 5, 50 - 64 Hz, (except for 60 Hz); Band 6, 66 - 84 Hz (Zemon et al., 2009).

Multilevel linear modeling (MLM). Multilevel linear modeling began with a null model. Participants were included as a random effect of intercept, allowing for an assessment of within-subject variability compared with between-subject variability. Multilevel linear models were employed to examine the degree of correlation of data within an individual and between-group differences in component, diagnosis, stimulus condition, and deletion. MLM allows the analysis of several points of data within individual participants. Factors can be added hierarchically to the model to identify their influence on the fit of the model. Another advantage of using this type of analysis is that MLM allows for the inclusion of discrete and continuous variables, modeled simultaneously.

The null model intraclass correlation coefficients (ICCs) were computed for the following variables: amplitude, latency, MSC, and ratio of amplitude from long- to short-conditions. ICCs greater than .05 suggest sufficient correlation or coherence of data within a participant to justify the use of a multilevel linear model. This indicates that data within a participant are more coherent than data across all participants. In the current study, the use of MLM is particularly useful in examining the fixed effect of diagnosis.

Chi-squared likelihood ratio tests (change in -2LL) were used to examine the improvement of the fit with the addition of each new fixed factor in the hierarchical model. As factors were added with each model, we expected smaller -2 log likelihood values, which indicate an improved fit. Main effects and interactions are reported as well.

Ratio of amplitude for long- to short-duration conditions. Past studies have relied on difference scores of amplitude for each component to measure if amplitude changes for each participant between the two conditions. The current study aimed to take into account the major

differences in overall amplitude between groups in order to provide a more accurate depiction of amplitude change between the standard and short conditions for each individual. To accomplish this, a new measure was employed that, instead of using difference scores, creates a ratio of amplitude, long condition- to short condition. If there is no difference in peak-to-trough amplitudes in long and short conditions, the ratio should be 1. If peak-to-trough amplitude is greater in the short condition as compared to the long condition, the ratio should be less than 1. Alternatively, if the peak-to-trough amplitude in the long condition is greater than in the short condition, the ratio should be greater than 1.

Power analysis. In a recent study, Zemon and Gordon (2017) introduce a novel technique for analyzing the frequency-domain. This method involves assessing the power of frequency bands. The bands used in the current study are the same used in the examination of MSC. A power analysis was conducted by extracting the amplitudes of the even harmonics of the response for each participant. Sum of squared amplitudes of the frequency components comprising each band (1-6) were computed for each individual. The total mean power of frequency components for each band was computed. This procedure was done for both the long and the short condition.

Zemon and Gordon (2017) provide support for this technique through the comparison of principal component analysis of frequency components responsible for the response with time-domain measures. In contrast to widely used time-domain analysis, which relies heavily on the subjective visual inspection of a waveform, this power band analysis provides an objective measure to assess the integrity of the visual pathway and characteristics of the response. Zemon and Gordon found that P60-N75 correlates most strongly with Bands 2 and 3, but also with Band 4, and N75-P100 amplitude correlates most strongly with Band 2. Band 1 correlates with P100-

N135 amplitude. P100 is pronounced in the reconstruction of the waveform when only frequencies of Band 2 are included. P100 can be considered to be derived from "intracortical GABAergic inhibitory" activity. Zemon, Kaplan, and Ratliff (1980) showed that application of bicuculline to the scalp not only attenuated the positive deflection P100, but also increased the negative amplitude of P60-N75. Because of this interplay and inter-dependency effects of excitation and inhibition on the amplitude of the peaks, a power analysis of the frequency components is a more objective measure of excitatory activity as compared relying on the subjective analysis of the peak-to-trough amplitudes of the earliest deflections. Zemon and Gordon (2017) also measure the ratio of power in each band from long- to short-duration conditions. This is also examined in the current paper.

Results

Amplitude. Mean values of amplitude and latency are reported in Table 1 (long condition) and Table 2 (short condition). Pairwise comparisons of a three-way interaction of Component x Stimulus x Diagnosis are shown in Table 4. There were some significant differences among groups of mean amplitude at some peak-to-trough deflections in the long condition. Examination of Figure 1 shows overlap of 95% confidence intervals at all peak-to-trough deflections except between TD and PMS groups at P60-N75 and N75-P100. TD and iASD confidence intervals do not overlap for N75-P100. These differences are significant at the .05 level. Pairwise comparisons also reveal the same significant differences in the short condition, as indicated by distinct 95% confidence intervals (see Figure 2).

Table 3 shows regression coefficients for a hierarchical MLM of amplitude. In Model 1, participant is a random intercept: this is the null model. In the null model, estimates of

covariance parameters revealed an intraclass correlation coefficient (ICC) of .32 ($p < .001$), indicating that participant as a variable accounted for a significant amount of the variance in amplitude**.** In Model 2, peak-to-trough deflection was included as a fixed factor resulting in a significant improvement in the fit of the model (Δ-2LL = 122.01, $\Delta df = 4$, $p < .001$). Peak-to-trough deflection was significant as a predictor of amplitude ($F(4,477) = 34.76$, $p < .001$). With the addition of the fixed effect, stimulus condition in Model 3, the fit of the model improved (Δ-2LL = 34.32, $\Delta df = 1$, $p < .001$). Stimulus condition explained a significant amount of the variance ($F(1, 477) = 35.59$, $p < .001$) and peak-to-trough deflection continued to be significant as a univariate effect after the addition of stimulus condition as a factor ($p < .001$). In Model 4, with the addition of diagnosis as a fixed factor, the model significantly improved (Δ-2LL = 14.68, $\Delta df = 2$, $p < .001$) ($F(2, 53) = 8.46$, $p < .001$). In Model 5, the following two-way interactions were added to the model; Peak-to-trough deflection x Stimulus, Peak-to-trough deflection x Diagnosis and Stimulus x Diagnosis, (Δ-2LL = 50.20, $\Delta df = 14$, $p <.001$) and the fit of the model improved significantly. However, only Peak-to-trough deflection x Dx was significant ($F(8, 477) = 6.01$, $p <. 001$. A three-way interaction was added in Model 6; Peak-to-trough deflection x Stimulus x Diagnosis. The interaction did not improve the fit of the model (Δ-2LL = 3.63, $\Delta df = 8$, $p > .05$).

Magnitude Squared Coherence. Pairwise comparisons of a three-way interaction of Diagnosis x Band x Stimulus for magnitude squared coherence in the long condition are shown in Table 6. Significant differences at the .05 level are clear though examination of the 95% confidence intervals of the TD group compared with the PMS group and the iASD compared with the PMS group for Band 1 (see Figure 3). All groups show significant differences from one another at

Band 2 and Band 3. At Band 4 TD is significant from both iASD and PMS. iASD and PMS confidence intervals overlap at Band 4. All groups overlap at Band 5 and Band 6.

In the short condition some of these differences are no longer significant (see Figure 4). In Band 1 all confidence intervals overlap. In Band 2 all groups are significantly different from one another. In Band 3 TD and iASD are significantly different and TD and PMS are significantly different but iASD and PMS overlap. Significant differences seen in the long condition in Band 4 are no longer present in the short condition. All groups overlap at Band 5 and Band 6.

Table 5 shows regression coefficients for a hierarchical MLM of MSC. In the null model, participant explained a significant amount of the variance of MSC giving an intraclass correlation coefficient (ICC) of .17 ($p < .001$), justifying the use of a mixed linear model analysis. In Model 2, band was included as a fixed factor resulting in a significant improvement in the fit of the model (Δ-2LL = 350.65, $\Delta df = 1$, $p < .001$). Band was a significant factor in predicting MSC ($F(5, 583) = 96.17$, $p < .001$). The fit of the model improved with the addition of stimulus condition as a fixed factor in Model 3 (Δ-2LL = 14.56, $\Delta df = 1$, $p < .001$), ($F(1, 583) = 14.74$, $p = .000$). The fit improved again in Model 4 with the addition of diagnosis as a fixed factor (Δ-2LL = 30.10, $\Delta df = 2$, $p < .001$), ($F(2, 53) = 20.27$, $p < .001$). In Model 5, the following two-way interactions were added to the model; Band x Stimulus condition, Band x Diagnosis, Stimulus condition x Diagnosis (Δ-2LL = 184.47, $\Delta df = 17$, $p < .001$). All interactions significantly improved the model fit; Band x Stimulus condition ($F(5, 583) = 2.6$, $p = .024$), Band x Diagnosis ($F(10, 583) = 17.36$, $p < .001$), Stimulus condition x Diagnosis ($F(2, 583) = 15.16$, $p < .001$). In Model 6, a three-way interaction of the interaction of Diagnosis x

Band x Stimulus condition was added. The interaction was not significant and did not improve the fit of the model (Δ-2LL = 12.17 Δ, *df* = 10, *p* >.05). The addition of this interaction resulted in an increase in significance of Band x Stimulus condition interaction; p-value changed from *p* = 0.02 to *p* = .006.

Latency. As apparent in examination of Figure 5 and Figure 6 there are no significant differences between group mean latency at any of the peak-to-trough deflections; this is also shown by overlapping 95% confidence intervals seen in Table 8. Table 7 shows regression coefficients for a hierarchical MLM of latency. In Model 1 (null model), participant is a random intercept. Participant explained a significant amount of the variance in latency. Estimates of covariance parameters revealed an intraclass correlation coefficient (ICC) of 0, showing correlated latency within participants**.** In Model 2, Stimulus condition was included as a fixed factor but did not improve the fit of the model (Δ-2LL = 0.002, Δ*df* = 1, *p* > .05). Stimulus condition was not a significant predictor of latency (*F*(1, 636) = .03, *p* = .87) With the addition of the fixed effect, peak-to-trough deflection in Model 3, the fit of the model improved (Δ-2LL = 1449.31, Δ*df* = 5, *p* < .001). Peak-to-trough deflection explained a significant amount of the variance (F(5, 636) = 1141.89, p < .001). In Model 4, with the addition of an interaction of Stimulus condition x Peak-to-trough deflection, the model did not significantly improve (Δ-2LL = 0.58, Δ*df* = 5, *p* >.05), F(5, 636) = .12, *p* = .99, *p* > .05. In Model 5, diagnosis was added as a fixed factor (Δ-2LL = 11.60, Δ*df* = 10, *p* > .05) and did not significantly improve fit. Diagnosis was not significant as a univariate effect (*F*(2, 636) = 2.07, *p* = .13).

Ratio of amplitude long- to short- conditions. Figure 4 shows all 95% confidence intervals overlap at each peak-to-trough-deflection. Table 9 shows regression coefficients for a

hierarchical MLM of the ratio the amplitude in the long condition to the short condition. In Model 1, participant is a random intercept. In the null model, estimates of covariance parameters revealed an intraclass correlation coefficient (ICC) of .17 ($p < .05$). In Model 2, peak-to-trough deflection was included as a fixed factor and did not result in a significant improvement in the fit of the model (Δ-2LL = 8.34, $\Delta df = 4$, $p = .08$). Peak-to-trough deflection was not a significant predictor of ratio *(*$F(4, 212) = 2.13$, $p = .08$). The addition of the fixed effect, diagnosis in Model 3 did not significantly improve the fit of the model (Δ-2LL = 2.06, $\Delta df = 2$, $p = .36$), ($F(2, 53) = 1.05$, $p = .36$). In Model 4, with the addition of an interaction of Peak-to-trough deflection x Diagnosis, the model did significantly improve (Δ-2LL = 21.568, $\Delta df = 8$, $p < .05$ or $p < .001$), ($F(8, 212) = 2.84$, $p = .005$). In Model 5, deletion was added as a fixed factor (Δ-2LL = 4.22, $\Delta df = 2$, $p > .05$) and did not significantly improve fit, ($F(2, 53) = 2.20$, $p = .12$).

Power. Additional analysis was done to assess the power of the frequency components of each band. Total mean power at the frequencies for each band are plotted for the long condition in Figures 8-11. The most notable difference in bands can be seen in Bands 1 and 2, where the TD group showed much greater power compared to both the iASD group and the PMS group. iASD power is also greater than PMS power in Bands 1 and 2 and is significantly more coherent. In Bands 3 and 4, power is again greatest for the TD group, but clearly reduced as compared with Band 1 and Band 2, which carry the most power. Band 4 power is greater for TD than iASD and PMS, and iASD and PMS are not distinct from one another (see Figure 10). In Band 5, the iASD and PMS groups have greater power as compared to the TD groups with PMS having the greatest power. Band 6 power is greatest in TD compared to PMS and iASD (which are not distinct from

one another) (see Figure 11). It must be acknowledged that these differences in Bands 5 and 6 are irrelevant as none of the groups reach the critical value for MSC in these bands.

For the short condition, the total mean power in frequency bands are presented in Figures 12-15. In the short condition, for TD Bands 1 and 2 have the most power, followed by iASD, and PMS has the least power; all groups are distinct from one another in these two bands. There is a large difference in power for Band 3, where TD has much greater power than both iASD and PMS. Power in Band 4 is also greatest for the TD group and there is no distinct difference in power for iASD and PMS (see Figure 14). Power in Bands 5 and 6 are irrelevant as none of the groups reach the critical value for MSC (see Figure 4 for MSC in the short condition).

Ratio of power in long- to short- duration conditions. For children in the TD group, the ratio of power in the long to the short condition goes from about equal between conditions, to the short condition having about double the amount of power as in the long condition, as frequencies move from low to high, and bands move from 1-6 (see Figure 16). Bands 1-3 have ratio scores of $M = 0.85$ (Band 1), $M = 0.96$ (Band 2), and $M = 1.18$ (Band 3). Bands 4-6 show much larger power in the short condition than the long condition, indicated by ratios of long- to short-duration conditions of $M = 0.53$ (Band 4), $M = 0.37$ (Band 5), and $M = 0.52$ (Band 6).

Both the iASD and PMS groups show an increase in band power in the short condition as compared to the long condition across all frequency bands. The iASD group had the following ratios: $M = 0.65$ (Band 1), $M = 0.71$ (Band 2), $M = 0.66$ (Band 3), $M = 0.55$ (Band 4), $M = 0.60$ (Band 5), $M = 0.56$ (Band 6). The PMS group had the following ratios: $M = 0.50$ (Band 1), $M = .59$ (Band 2), $M = 0.52$ (Band 3), $M = 0.59$ (Band 4), $M = 0.59$ (Band 5), and $M = 0.54$ (Band 6).

Discussion

Amplitude. MLM revealed that amplitude of the response was affected by stimulus condition and diagnosis. Examination of Figure 1 and 2 illustrates the differences between the groups within each condition, long and short. As seen in Figure 1, 95% confidence intervals for TD and PMS do not overlap at P60-N75 and no groups overlap at N75-P100.

In a past study, Siper et al. (2016) found decreased P60-N75 and N75-P100 amplitudes in an iASD group relative to a TD groups. Siper et al. suggest that this indicates decreased excitatory input to the cortex, indicated by decreased P60-N75 amplitude. This decreased amplitude results in a proportional loss of inhibition, noted by decreased N75-P100 amplitude. Siper et al. state that because this loss is proportional, it can be understood that there is no deficit in intracortical inhibition.

Principal component analysis by Zemon and Gordon (2017) showed a high concordance in P60-N75 amplitude with power in Bands 2-4. Bands 2-4 were correlated with P60-N75/N75-P100 amplitudes, indicating they result from early activity. P100-N135 amplitude loaded with Band 1 power, indicating that it reflects low frequency inhibitory, late activity. Interestingly, P100-N135 amplitude was where differences between the TD group and the iASD and PMS groups were no longer distinct or significant, providing additional support that intracortical inhibitory activity is intact in autism.

MSC. Siper et al. (2016) found significant univariate main effects for Bands 2-5 in the long condition and Bands 2 and 3 in the short condition for TD and iASD groups. Examination of Figure 3 shows that, in the long condition, all three groups are significantly different from one another for Bands 2 and 3. For Band 1, iASD and TD do not differ significantly, but both differ

significantly from PMS at the .05 level. For Band 4, TD confidence intervals do not overlap with iASD or PMS groups, indicating significant differences at the .05 level.

In the short condition, Figure 4 shows that differences previously seen for Band 1 in the long condition no longer reach significance. For Band 2, all groups are significantly different at the .05 level. For Band 3, iASD and PMS are no longer distinct from one another, though TD and PMS are distinct. This maintained difference for Bands 2 and 3 suggest a continued deficit in high frequency excitatory activity in the short condition for the groups with ASD.

Latency. The multilevel linear models, Figures 5 and 6, clearly show no effect of condition or group on latency. This same preservation of latency was found by Siper et al. (2016). Siper et al. found no difference in group latencies among TD, iASD, and a group of unaffected siblings of children with iASD at the measured peak-to-trough deflections (P60, N75, and P100). The current study replicates these findings and adds that there are no latency differences at later peaks (N135, P200, and N250) suggesting no delay in information transmission to the cortex.

Ratio of amplitude in long- to short-duration conditions. While the addition of diagnosis as a main effect did not improve the fit of the model, the interaction of Peak-to-Trough Deflection x Diagnosis was significant. Figure 7 shows no significant difference in ratios between groups at the .05 level, however, the least overlap of 95% confidence intervals can be seen for P100-N135 amplitude between the TD and PMS groups, and also between iASD and PMS groups for P200-N250 amplitude. TD ratios remain around 1 for all peak-to-trough deflections, meaning that peak-to-trough amplitudes in the long condition and short condition are comparable in magnitude. The ratios for iASD fall below 1 but are generally around the same value $M = 0.83$, ranging from 0.74-0.84, more differences can be seen between the long and short conditions in

later peak-to-trough deflections for the iASD group (short being larger in amplitude than long). PMS ratios change the most dramatically across deflections in the VEP waveform. It is particularly notable that the ratio of amplitude of long- to short-duration conditions decreases to $M = 0.50$ for P100-N135amplitude, indicating that in the short condition, P100-N135 amplitude is about twice as large as it is in the long condition.

Band Power. Past studies of spectra power in iASD report increased power at high frequencies (30-80 Hz) as compared to TD populations (Yizhar, 2011). The current results suggest the opposite trend in power spectra. Here we report decreased power in iASD and PMS groups as compared to the TD group in frequencies across all bands. Though in PMS there is a relative increase in power in Band 5 (in the long condition) and Band 6 (in the short condition) as compared to TD and iASD groups (see Figures 11 and 15), magnitude squared coherence analyses reveal that none of these bands for the PMS group reach their respective critical values. In the PMS group Bands 3-6 and have a very low *signal to noise ratio* (SNR) and thus the power is more likely attributed to high levels of neural noise than to an actual signal (see Figures 3 and 4).

Ratio of Power. Zemon and Gordon (2017) found that the ratio of power in long- to short-duration conditions decreases (that is power is greater in long conditions) moving from low to high frequencies. This may reflect a greater effect of adaptation for early excitatory activity in typical individuals. This effect can be seen in the current study for the TD group, but not the iASD and PMS groups.

For the TD group, power was found to be much greater for excitatory activity in the short condition. This may reflect an adaptation effect caused by prolonged exposure to the stimulus in the long condition.

Interestingly, the iASD and PMS groups show a ratio of ~ 0.5 from long:short conditions across all bands indicating that the short condition results in greater power across all frequencies. As illustrated by Figure 14, both the TD group and the iASD and PMS groups adapt at high frequencies from the short to the long condition. However, the iASD and PMS groups show adaptation the across both high and low frequencies. This could tentatively be interpreted as both excitation and inhibition showing adaptation effects, and the TD group only showing adaptation effects in high frequency excitatory activity.

Contributions of the current study. This is the first study to apply the measure of total mean power of frequency bands, established by Zemon and Gordon (2017), to atypical populations. This is an objective measure of the visual evoked response. In addition, this study provides support for the following two claims:

1. In both iASD and PMS, excitatory input is affected while inhibitory activity remains intact providing support for the altered E/I profile model of ASD, but *not* in the direction that Rubenstein and Merzenich (2003) propose.
2. Visual attention is potentially intact in both PMS and iASD. Attending improves in the shorter condition, particularly so in the PMS group.

Model of E/I in iASD. In the current study, the inclusion of a genetically-defined subtype of ASD related to deletion or mutation in a gene implicated in excitatory functioning (PMS group) and its comparison with idiopathic ASD provides a unique opportunity by which to examine the

model of E/I in autism. What is responsible for the altered E/I balance in iASD, excitation or inhibition?

Effects of deletions and mutations in the *SHANK3* gene have revealed *SHANK3* as a causal gene in Phelan-McDermid syndrome. Shank3 proteins have been shown to be important in the development of postsynaptic density of excitatory synapses. Shank3 proteins are crucial in establishing synaptogenesis and in the maintenance and plasticity of these synapses. These proteins also play a role in "postsynaptic signal transduction" (Harony, Günal, & Buxbaum, 2013, p 438).

In the current study individuals Phelan-McDermid syndrome show a significant decrease in frequency bands and peak-to-trough deflections thought to reflect excitatory input, as compared to TD controls, and to a lesser degree, the iASD group. This suggests that the current electrophysiological examinations show that decreased excitatory input are consistent with studies in model systems demonstrating the deleterious effects of SHANK3 deficiency on glutamatergic activity (Bozdagi et al., 2010). We see the same physiological pattern in individuals with iASD in our data however, to a lesser degree, suggesting that a deficit in excitation may be the common denominator in the two disorders.

N135. The findings of the current study suggest that though excitatory input to the cortex may be decreased in autism, inhibition in the cortex is affected by the long condition but potentially preserved in the short condition. These findings also suggest that attentional mechanisms seem to be intact and perhaps even enhanced in the short condition. P100-N135 amplitude is correlated with Band 1. The ratios of P100-N135 amplitudes in iASD and PMS groups show greater amplitudes for this deflection in the short condition, supported by the finding that differences

between groups in Band 1 coherence in the long condition are no longer present for Band 1 in the short condition.

Both P100 and N135 have been shown to be modulated by visual attending. Vogel and Luck (2000) propose that P100 and N135 are associated with sensory gating. Vogel and Luck suggest that the modulation of P100 amplitude reflects suppression of processing while N135 reflects enhancement, both modulations resulting from attentional orienting. Natale, Marzi, Girelli, Pavone, and Pollman (2006) suggest that the N135 effect might represent a transient allocation of attention captured by the appearance of the stimulus, which may explain why N135 is enhanced for the short condition. N135 may be modulated by a shift of attention elicited by relevant stimuli. This has been interpreted as evidence that N135 indexes attentional shifts, while P100 may be useful as an index of pre-attentive arousal or endogenous (as opposed to exogenous) attention.

Whether the current results reflect normal attending or enhanced attending based in visual discrimination is unclear. There were no significant differences in P100-N135 amplitude between groups for the long or short condition, suggesting intact attention across groups. However, the iASD and PMS groups show a large proportional increase in amplitude at P100-N135 from the long to the short condition (as indexed by the ratio of amplitude measure) while the amplitude ratio at P100-N135 for the TD group is around 1 (there is not much change from the long condition to the short). Is this an indication of enhanced visual attention in the short condition, particularly for the PMS group?

Further research should examine the concordance of these P100-N135 effects with behavioral manifestations. Deletion size and presence of an ASD diagnosis in the PMS group

was not discussed in this paper, however, further investigations should include those factors in analyses. Limitations of the current study should be addressed and minimized in future conditions, mainly, the small sample size, particularly for the TD group (n = 12). The use of medications is a potential confound (many of the Phelan-McDermid syndrome children were on anti-consultants for epilepsy). IQ should also be taken into account for this study as it is variable for children with autism and all of the Phelan-McDermid syndrome children were also diagnosed with intellectual disability.

The greatest contribution of the current study is the application of an objective measure of the visual evoked potential within the frequency domain to a population of individuals with ASD and PMS. The power analysis employed here reveals clear differences between the groups that align with the differences seen in the time domain. This measure, developed by Zemon and Gordon (2017), demosntrates the potential to identify potential biomarkers of ASD.

References

Betancur, C. (2011). Etiological heterogeneity in autism spectrum disorders: More than 100 genetic and genomic disorders and still counting. *Brain Research, 1380*, 42-77.

Blatt, G., (2013). Inhibitory and Excitatory Systems in Autism Spectrum Disorders. In Buxbaum, J., Hof, P (Eds.),Waltham, MA: Elsevier Inc. *The Neuroscience of Autism Spectrum Disorders*, (pp. 335–346).

Blatt, G., Fitzgerald, C., Guptill, J., Booker, A., Kemper, T., & Bauman, M. (2001). Density and distribution of hippocampal neurotransmitter receptors in autism: An autoradiographic study. *Journal of Autism and Developmental Disorders, 31*(6), 537-43.

Bozdagi, O., Sakurai, T., Papapetrou, D., Wang, X., Dickstein, D. L., Takahashi, N., … Buxbaum, J. D. (2010). Haploinsufficiency of the autism-associated *Shank3* gene leads to deficits in synaptic function, social interaction, and social communication. *Molecular Autism*, *1*, 15. http://doi.org/10.1186/2040-2392-1-15

Buxbaum, J. (2009). Multiple rare variants in the etiology of autism spectrum disorders. *Dialogues in Clinical Neuroscience, 11*(1), 35-43.

Christensen, D., Baio, J., Braun, K. (2016). Prevalence and Characteristics of Autism Spectrum Disorder Among Children Aged 8 Years. Autism and Developmental Disabilities Monitoring Network, 11 Sites, United States, 2012. MMWR Surveill Summ. 65(No. SS-3)(No. SS-3):1–23. DOI: http://dx.doi.org/10.15585/mmwr.ss6503a1.

Costales, J. L., & Kolevzon, A. (2015). Phelan–McDermid Syndrome and *SHANK3*: Implications for Treatment. *Neurotherapeutics*, *12*(3), 620–630. http://doi.org/10.1007/s13311-015-0352-z

Creel, D. (2012) Visually Evoked Potentials. In: Kolb H, Fernandez E, Nelson R, editors. Webvision: The Organization of the Retina and Visual System [Internet]. Salt Lake City (UT): University of Utah Health Sciences Center; 1995-. Available from: https://www.ncbi.nlm.nih.gov/books/NBK107218/

Di Russo F., Martínez A., Sereno M., Pitzalis S., Hillyard S. (2002) Cortical sources of the early components of the visual evoked potential. Hum Brain Mapp. 15(2):95-111

Di Russo, F., Pitzalis, S., Spitoni, G., Aprile, T., Patria, F., Spinelli, D. & Hillyard, S.A. (2005) Identification of the neural sources of the pattern-reversal VEP. *Neuroimage*, **24**, 874-886.

DSM-5. 5th Edition. Washington, DC: American Psychiatric Association (2013). American Psychiatric Association. Diagnostic and Statistical Manual of Mental Disorders.

Georgiades, S., Szatmari, P., Boyle, M., Hanna, S., Duku, E., Zwaigenbaum, L., Bryson, S. Fombonne, E. Volden, J., Mirenda, P., Smith, I., Roberts, W., Vaillancourt. T., Waddell, C., Bennett, T., Thompson, A. (2013). Investigating phenotypic heterogeneity in children with autism spectrum disorder: A factor mixture modeling approach. *Journal of Child Psychology and Psychiatry, 54*(2), 206-215.

Harony, H., Günal, O. & Buxbaum, J. (2013), SHANK2 and SHANK3 Mutations Implicate Glutamate Signaling Abnormalities in Autism Spectrum Disorders, In Buxbaum, J., Hof, P (Eds.),Waltham, *The Neuroscience of Autism Spectrum Disorders*, pp. 427–447.

Harony-Nicolas, H., De Rubeis, S., Kolevzon, A., Buxbaum, J., & Maria, B.(2015).Phelan-McDermid syndrome. *Journal of Child Neurology, 30*(14), 1861-1870.

Hussman, J. (2001). Suppressed GABAergic inhibition as a common factor in suspected etiologies of autism. *Journal of Autism and Developmental Disorders, 31*(2), 247-8.

Kim S. and Lord, C., (2013). The behavioral manifestations of autism spectrum disorders, In Buxbaum, J., Hof, P (Eds.),Waltham, *The Neuroscience of Autism Spectrum Disorders*, (pp. 25–37).

Lord, C., DiLavore, P. C., Gotham, K., Guthrie, W., Luyster, R. J., Risi, S., Rutter, M., ... (2012). Western Psychological Services (Firm). Autism diagnostic observation schedule: ADOS-2. Los Angeles, Calif: Western Psychological Services.

Natale, E., Marzi, C., Girelli, M., Pavone, E., & Pollmann, S. (2006). ERP and fMRI correlates of endogenous and exogenous focusing of visual-spatial attention. *European Journal of Neuroscience, 23*(9), 2511-2521.

Disorder Using Transient Visual Evoked Potentials. *PLoS ONE, 11*(10), E0164422.

Rubenstein, J., & Merzenich, M. (2003). Model of autism: Increased ratio of excitation/inhibition in key neural systems. *Genes, Brain and Behavior, 2*(5), 255-267.

Rutter, M., LeCouteur, A., Lord, C. (2008). Autism Diagnostic Interview – Revised. Los Angeles: Western Psychological Services.

Siper, P., Zemon, V., Gordon, J., George-Jones, J., Lurie, S., Zweifach, J., . . . Kolevzon, A. (2016). Rapid and Objective Assessment of Neural Function in Autism Spectrum

Shigeto, H., Tobimatsu, S., Yamamoto, T., Kobayashi, T., & Kato, M. (1998). Visual evoked cortical magnetic responses to checkerboard pattern reversal stimulation: A study on the neural generators of N75, P100 and N145. *Journal of the Neurological Sciences,156*(2), 186-194.

Soorya, L., Kolevzon, A., Zweifach, J., Lim, T., Dobry, Y., Schwartz, L.,…Buxbaum, J. (2013). Prospective investigation of autism and genotype-phenotype correlations in 22q13 deletion syndrome and SHANK3 deficiency. *Molecular Autism.*

Vogel, E., & Luck, S. (2000). The visual N1 component as an index of a discrimination process. *Psychophysiology,37*(2), 190-203.

Yizhar, O., Fenno, L., Prigge, M., Schneider, F., Davidson, T., O'Shea, D., . . . Deisseroth, K. (2011). Neocortical excitation/inhibition balance in information processing and social dysfunction. *Nature, 477*(7363), 171-8.

Zemon, V. & Gordon, J. Quantification and Statistical Analysis of the Transient Visual Evoked Potential to a Contrast-Reversing Pattern: A Frequency Domain Approach *European Journal of Neuroscience*. Submitted, 2017.

Zemon, V., Gordon, J., O'Toole, L., Monde, K., Dolzhanskaya, V., Shapovalova, V., Hu, J., Furhman, J., Granader , Y. (2009). Transient Visual Evoked Potentials (tVEPs) to Contrast-Reversing Patterns: A Frequency Domain Analysis. *Invest. Ophthalmol. Vis. Sci.* 50(13):5880.

Zemon, V., Kaplan, E., & Ratliff, F. (1980). Bicuculline enhances a negative component and diminishes a positive component of the visual evoked cortical potential in the cat. *Proceedings of the National Academy of Sciences of the United States of America*, *77*(12), 7476–7478.

Table 1. Amplitude and Latency

	Long Condition										
	Amplitude (μV)					***Latency (ms)***					
Group	***P60-N75***	***N75-P100***	***P100-N135***	***N135-P200***	***P200-N250***	***P60***	***N75***	***P100***	***N135***	***P200***	***N250***
TD	16.25	28.96	18.38	8.68	12.94	51.25	68.67	97.08	155.42	196.33	266.25
	(2.68)	(3.32)	(4.01)	(1.39)	(2.65)	(1.48)	(0.83)	(2.57)	(8.48)	(10.02)	(11.68)
iASD	8.48	17.24	13.95	9.525	8.98	52.79	70.79	101.12	150.04	205	267.38
	(1.10)	(1.80)	(1.51)	(1.06)	(1.10)	(1.34)	(1.30)	(1.52)	(4.50)	(5.79)	(7.90)
PMS	5.59	12.53	10.78	5.829	6.63	48.43	70.14	102.48	152.81	211.38	263.29
	(0.63)	(1.81)	(2.04)	(1.09)	(0.85)	(0.37)	(0.36)	(0.42)	(1.25)	(1.61)	(2.19)

Note: Mean values (standard error of the mean) for the long condition (60-s contrast-reversing checkerboard).

Table 2. Amplitude and Latency

	Short Condition										
	Amplitude (μV)					***Latency (ms)***					
Group	***P60-N75***	***N75-P100***	***P100-N135***	***N135-P200***	***P200-N250***	***P60***	***N75***	***P100***	***N135***	***P200***	***N250***
TD	19.45	32.64	18.98	12.02	14.59	50.75	68.50	95.00	150.50	193.67	257.33
	(4.29)	(6.22)	(4.76)	(2.19)	(2.39)	(1.40)	(0.79)	(2.34)	(9.57)	(10.45)	(8.99)
iASD	11.363	22.46	19.19	14.07	14.31	52.38	70.1	98.9	150.4	205.5	267.1
	(1.84)	(3.05)	(2.50)	(1.98)	(2.04)	(1.05)	(1.26)	(1.64)	(3.91)	(5.43)	(6.75)
PMS	4.965	14.99	17.64	10.44	6.44	53.3	68.2	105	166.3	223.9	271.5
	(1.03)	(2.23)	(2.19)	(1.93)	(1.26)	(2.17)	(2.94)	(5.95)	(7.83)	(9.95)	(13.83)

Note: Mean values (standard error of the mean) for the short condition contrast-reversing checkerboard (ten trials of 3-s epochs).

Table 3. Multilevel Linear Models for Amplitude (n = 53)

	Regression coefficients (estimates of fixed effects)					
Effect	Model 1 (null)	Model 2	Model 3	Model 4	Model 5	Model 6
Intercept	13.50 (.94)***	10.39 (1.17)***	12.40 (1.21)***	8.16 (1.64)***	7.71 (2.02)***	6.65(2.22)**
Main effects						
Peak-to-trough-deflection						
P60-N75	—	-.51(1.10)	-.51(1.06)	-.51(1.06)	.-2.37(2.05)	-1.91(2.51)
N75-P100	—	9.68(1.10)***	9.68(1.06)***	9.68(1.06)***	7.49(2.05)***	8.76(2.51)**
P100-N135	—	6.23(1.10)***	6.23(1.06)***	6.23(1.06)***	9.45(2.05)***	11.66(2.51)***
N135-P200	—	.13(1.10)	.13(1.10)	.13(1.10)	-2.93(2.05)	4.28(2.51)
P200-N250	—	0[a]	0[a]	0[a]	0[a]	0[a]
Stimulus condition						
Long condition	—	—	-.03(.01)***	-4.01(.67)***	-2.95(1.70)	-.84(2.51)
Short condition	—	—	0[a]	0[a]	0[a]	0[a]
Dx						
TD	—	—	—	9.19(2.26)***	6.88(2.99)*	7.94(3.46)*
iASD	—	—	—	4.77(1.90)*	5.85(2.51)*	7.66(2.91)**
PMS	—	—	—	0[a]	0[a]	0[a]
Two-way interactions						
Peak-to-trough deflection x Stimulus condition						
P60-N75 x Long condition	—	—	—	—	.68(2.02)	-.25(3.56)
P60-N75 x Short condition	—	—	—	—	0[a]	0[a]
N75-	—	—	—	—	-1.81(2.02)	-4.35(3.55)

P100 x Long condition						
N75-P100 x Short Condition	—	—	—	—	0[a]	0[a]
P100-N135 x Long condition	—	—	—	—	-2.31(2.02)	-6.72(3.56)
P100-N135 x Short condition	—	—	—	—	0[a]	0[a]
N135-P200 x Long condition	—	—	—	—	-1.37(2.02)	-4.06(3.55)
N135-P200 x Short condition	—	—	—	—	0[a]	0[a]
P200-N250 x Long condition	—	—	—	—	0[a]	0[a]
P200-N250 x Short condition	—	—	—	—	0[a]	0[a]
Peak-to-Trough Deflection x Diagnosis						
P60-N75 x TD					6.11(2.77)*	6.77(3.90)
P60-N75 x iASD					.31(2.33)	-1.03(3.28)
P60-N75 x PMS					0[a]	0[a]
N75-P100 x TD					10.44(2.77)***	9.29(3.90)*
N75-P100 x iASD					1.61(2.33)	-.61(3.28)
N75-					0[a]	0[a]

P100 x PMS		
P100-N135 x TD	-2.83(2.77)	-6.18(3.90)
P100-N135 x iASD	-3.17(2.33)	-6.36(3.28)
P100-N135 x PMS	0[a]	0[a]
N135-P200 x TD	-5.44(2.77)	-6.85(3.90)
N135-P200 x iASD	-1.94(2.33)	-4.22(3.28)
N135-P200 x PMS	0[a]	0[a]
P200-N250 x TD	0[a]	0[a]
P200-N250 x iASD	0[a]	0[a]
P200-N250 x PMS	0[a]	0[a]
Stimulus condition x Diagnosis		
Long condition x TD	1.29(1.75)	-.81(3.90)
Long condition x iASD	-.87(1.47)	-4.49(3.28)
Long condition x PMS	0[a]	0[a]
Short condition x TD	0[a]	0[a]
Short condition x iASD	0[a]	0[a]
Short condition x PMS	0[a]	0[a]

Three-way interactions						
Band x Stimulus condition x Diagnosis						
P60-N75 x Long condition x TD	—	—	—	—	—	-1.30(5.52)
P60-N75 x Long condition x iASD	—	—	—	—	—	2.69(4.64)
P60-N75 x Long condition x PMS	—	—	—	—	—	0[a]
P60-N75 x Short condition x TD						0[a]
P60-N75 x Stimulus condition						0[a]
P60-N75 x Short condition x iASD	—	—	—	—	—	0[a]
P60-N75 x Short condition x PMS	—	—	—	—	—	0[a]
N75-P100 x Long condition x TD	—	—	—	—	—	2.32(5.52)
N75-P100 x Long condition x iASD	—	—	—	—	—	4.46(4.64)
N75-P100 x Long condition x	—	—	—	—	—	0[a]

PMS						
N75-P100 x Short condition x TD	—	—	—	—	—	0[a]
N75-P100 x Short condition x iASD	—	—	—	—	—	0[a]
N75-P100 x Short condition x PMS	—	—	—	—	—	0[a]
P100-N135 x Long condition x TD	—	—	—	—	—	6.71(5.52)
P100-N135 x Long condition x iASD	—	—	—	—	—	6.38(4.64)
P100-N135 x Long condition x PMS	—	—	—	—	—	0[a]
P100-N135 x Short condition x TD						
P100-N135 x Short condition x iASD						
P100-N135 x Short condition x PMS	—	—	—	—	—	0[a]
N135-	—	—	—	—	—	2.81(5.52)

P200 x Long condition x TD						
N135-P200 x Long condition x iASD	—	—	—	—	—	4.55(4.64)
N135-P200 x Long condition x PMS	—	—	—	—	—	0[a]
N135-P200 x Short condition x TD						0[a]
N135-P200 x Short condition x iASD						0[a]
N135-P200 x Short condition x PMS						0[a]
P200-N250 x Long condition x TD						0[a]
P200-N250 x Long condition x iASD						0[a]
P200-N250 x Long condition x PMS						0[a]
P200-N250 x Short						0[a]

condition x TD						
P200-N250 x Short condition x iASD						0[a]
P200-N250 x Short condition x PMS						0[a]
P200-N250 x Long condition x TD						0[a]
Variance components (random effects)						
Model Summary						
-2LL[b]	3939.84	3817.83	3783.51	3768.83	3718.63	3715.00
Estimated parameters	3	7	8	10	24	32

Note. Standard errors for parameter estimates are listed in parentheses.[a]The parameter is set to zero because it is redundant, cross-level interactions with redundant parameters are excluded from the table.

[b]-2LL; -2 log-likelihood is a measure of how well the model fits the data. Smaller numbers reflect a better fit.

* $p < .05$. ** $p < .01$. *** $p < .001$.

Table 4. Peak-to-Trough Amplitude x Stimulus Condition x Diagnosis

						95% Confidence Interval	
Peak-to-Trough Amplitude			*M*	*SE*	*df*	Lower Bound	Upper Bound
P60-N75	Long Condition	TD	16.250	2.647	242.733	11.036	21.464
		iASD	8.479	1.872	242.733	4.792	12.166
		PMS	3.659	2.224	242.733	-.722	8.040
	Short Condition	TD	19.450	2.647	242.733	14.236	24.664
		iASD	11.363	1.872	242.733	7.675	15.050
		PMS	4.741	2.224	242.733	.360	9.122
N75-P100	Long Condition	TD	28.958	2.647	242.733	23.744	34.173
		iASD	17.238	1.872	242.733	13.550	20.925
		PMS	10.229	2.224	242.733	5.848	14.610
	Short Condition	TD	32.642	2.647	242.733	27.427	37.856
		iASD	22.458	1.872	242.733	18.771	26.145
		PMS	15.418	2.224	242.733	11.037	19.799
P100-N135	Long Condition	TD	18.408	2.647	242.733	13.194	23.623
		iASD	13.950	1.872	242.733	10.263	17.637
		PMS	10.759	2.224	242.733	6.378	15.140
	Short Condition	TD	20.067	2.647	242.733	14.852	25.281
		iASD	19.608	1.872	242.733	15.921	23.295
		PMS	18.312	2.224	242.733	13.931	22.693
N135-P200	Long Condition	TD	9.117	2.647	242.733	3.902	14.331
		iASD	9.525	1.872	242.733	5.838	13.212
		PMS	6.029	2.224	242.733	1.648	10.410
	Short Condition	TD	12.017	2.647	242.733	6.802	17.231
		iASD	14.367	1.872	242.733	10.680	18.054
		PMS	10.929	2.224	242.733	6.548	15.310
P200-N250	Long Condition	TD	12.942	2.647	242.733	7.727	18.156
		iASD	8.983	1.872	242.733	5.296	12.670
		PMS	5.818	2.224	242.733	1.437	10.199
	Short Condition	TD	14.592	2.647	242.733	9.377	19.806
		iASD	14.308	1.872	242.733	10.621	17.995
		PMS	6.653	2.224	242.733	2.272	11.034

Note: Dependent variable: amplitude.

Table 5. Multilevel Linear Models for Magnitude Squared Coherence (n = 53)

	Regression coefficients (estimates of fixed effects)					
Effect	Model 1 (null)	Model 2	Model 3	Model 4	Model 5	Model 6
Intercept	.22(.01)***	.10(.01)***	.09(.02)***	.03(.02)***	.12(.02)***	.11 (.03)***
Main effects						
Band						
Band 1	—	.21(.02)***	.21(.02)***	.21(.02)***	.13(.03)***	.15 (.03)***
Band 2	—	.24(.02)***	.24(.02)***	.24(.02)***	.06(.03)*	.08(.03)*
Band 3	—	.16 (.02)***	.16 (.02)***	.16 (.02)***	.02(.03)	.05(.03)
Band 4	—	.06(.02)***	.06(.02)***	.06(.02)***	.01(.03)	.01(.03)
Band 5	—	-.00(.02)	-.00(.02)	-.00(.02)	.01(.03)	.01(.03)
Band 6	—	0[a]	0[a]	0[a]	0[a]	0[a]
Stimulus Condition						
Long	—	—	-.03(.01)***	-.03(.01)***	-.04(.02)	-.02(.03)
Condition						
Short	—	—	0[a]	0[a]	0[a]	0[a]
Condition						
Dx						
TD	—	—	—	.15(.02)***	-.04(.03)	-.01(.04)
iASD	—	—	—	.06(.02)**	-.02(.03)	-.02(.03)
PMS	—	—	—	0[a]	0[a]	0[a]
Two-way interactions						
Bands x Stimulus Condition						
Band 1 x Long	—	—	—	—	.02(.03)	-.01(.05)
Condition						
Band 1 x Short	—	—	—	—	0[a]	. 0[a]
Condition						
Band 2 x Long	—	—	—	—	.07 (.03)*	.02(.05)
Condition						
Band 2 x Short	—	—	—	—	0[a]	. 0[a]
Condition						
Band 3 x Long	—	—	—	—	.06(.03)*	.01(.05)
Condition						
Band 3 x Short	—	—	—	—	0[a]	0[a]
Condition						
Band 4 x Long	—	—	—	—	.02(.03)	.01(.05)
Condition						
Band 4 x Short	—	—	—	—	0[a]	0[a]

Condition						
Band 5 x Long	—	—	—	—		.01(.05)
Condition					-.00(.03)	
Band 5 x Short	—	—	—	—	0[a]	0[a]
Condition						
Band 6 x Long	—	—	—	—	0[a]	0[a]
Condition						
Band 6 x Short	—	—	—	—	0[a]	0[a]
Condition						
Bands x						
Diagnosis						
Band 1 x TD					.10(.04)**	.08(.05)
Band 1 x iASD					.09(.03)**	.07(.04)
Band 1 x PMS					0[a]	0[a]
Band 2 x TD					.32(.04)***	.26(.05)***
Band 2 x iASD					.18(.03)***	.15(.04)***
Band 2 x PMS					0[a]	0[a]
Band 3 x TD					.29(.04)***	.20(.05)***
Band 3 x iASD					.09(.03)**	.07(.04)**
Band 3 x PMS					0[a]	0[a]
Band 4 x TD					.10(.04)**	.07(.05)
Band 4 x iASD					.04(.03)	.05(.04)
Band 4 x PMS					0[a]	0[a]
Band 5 x TD					-.02(.04)	-.01(.05)
Band 5 x iASD					-.02(.03)	-.01(.04)
Band 5 x PMS					0[a]	0[a]
Band 6 x PMS					0[a]	0[a]
Band 6 x PMS					0[a]	0[a]
Band 6 x PMS					0[a]	0[a]
Stimulus						
condition x						
Diagnosis						
Long condition x TD					.11(.02)***	.05(.05)
Long condition x iASD					.05(.02)**	.03(.04)
Long condition x PMS					0[a]	0[a]
Short condition x TD					0[a]	0[a]
Short condition x iASD					0[a]	0[a]
Short condition x PMS					0[a]	0[a]
Three-way interactions						
Band x Stimulus						

condition x Diagnosis						
Band 1 x Long condition x TD	—	—	—	—	—	.05(.07)
Band 1 x Long condition x iASD	—	—	—	—	—	.05(.06)
Band 1 x Long condition x PMS	—	—	—	—	—	0[a]
Band 1 x Short condition x TD						0[a]
Band 1 x Stimulus condition						0[a]
Band 1 x Short condition x iASD	—	—	—	—	—	0[a]
Band 1 x Short condition x PMS	—	—	—	—	—	0[a]
Band 2 x Long condition x TD	—	—	—	—	—	.11(.07)
Band 2 x Long condition x iASD	—	—	—	—	—	.05(.06)
Band 2 x Long condition x PMS	—	—	—	—	—	0[a]
Band 2 x Short condition x TD	—	—	—	—	—	0[a]
Band 2 x Short condition x iASD	—	—	—	—	—	0[a]
Band 2 x Short condition x PMS	—	—	—	—	—	0[a]
Band 3 x Long condition x TD	—	—	—	—	—	.17(.07)*
Band 3 x Long condition x iASD	—	—	—	—	—	.04(.06)
Band 3 x Long condition x PMS	—	—	—	—	—	0[a]
Band 3 x Short condition x TD						
Band 3 x Short condition x iASD						
Band 3 x Short condition x PMS	—	—	—	—	—	0[a]
Band 4 x Long condition x TD	—	—	—	—	—	.04(.07)
Band 4 x Long condition x iASD	—	—	—	—	—	-.01(.06)
Band 4 x Long condition x PMS	—	—	—	—	—	0[a]

Band 4 x Short condition x TD						0[a]
Band 4 x Short condition x iASD						0[a]
Band 4 x Short condition x PMS						0[a]
Band 5 x Long condition x TD						-.02(.07)
Band 5 x Long condition x iASD						-.02(.06)
Band 5 x Long condition x PMS						0[a]
Band 5 x Short condition x TD						0[a]
Band 5 x Short condition x iASD						0[a]
Band 5 x Short condition x PMS						0[a]
Band 6 x Long condition x TD						0[a]
Band 6 x Long condition x iASD						0[a]
Band 6 x Long condition x PMS						0[a]
Band 6 x Short condition x TD						0[a]
Band 6 x Short condition x iASD						0[a]
Band 6 x Short condition x PMS						0[a]
Variance components (random effects)						
Model Summary						
-2LL[b]	-533.40	-884.05	-898.61	-928.71	-1113.18	-1125.35
Estimated parameters	3	8	9	11	28	38

Note. Standard errors for parameter estimates are listed in parentheses.
[a]The parameter is set to zero because it is redundant, cross-level interactions with redundant parameters are excluded from the table.
[b]-2LL; -2 log-likelihood is a measure of how well the model fits the data. Smaller numbers reflect a better fit.
* $p < .05$. ** $p < .01$. *** $p < .001$.

Table 6. Frequency Band x Stimulus Condition x Diagnosis

Frequency bands			*M*	*SE*	*df*	95% Confidence Interval Lower Bound	95% Confidence Interval Upper Bound
Band 1	Long Duration	TD	.402	.031	365.231	.341	.464
		iASD	.358	.022	365.231	.315	.402
		PMS	.230	.026	365.231	.178	.281
	Short Duration	TD	.330	.031	365.231	.269	.392
		iASD	.314	.022	365.231	.270	.358
		PMS	.261	.026	365.231	.209	.313
Band 2	Long Duration	TD	.605	.031	365.231	.544	.667
		iASD	.408	.022	365.231	.364	.451
		PMS	.190	.026	365.231	.138	.242
	Short Duration	TD	.444	.031	365.231	.382	.505
		iASD	.328	.022	365.231	.284	.371
		PMS	.193	.026	365.231	.141	.245
Band 3	Long Duration	TD	.564	.031	365.231	.503	.626
		iASD	.267	.022	365.231	.224	.311
		PMS	.148	.026	365.231	.096	.199
	Short Duration	TD	.351	.031	365.231	.289	.412
		iASD	.215	.022	365.231	.171	.258
		PMS	.161	.026	365.231	.109	.212
Band 4	Long Duration	TD	.276	.031	365.231	.215	.338
		iASD	.168	.022	365.231	.125	.212
		PMS	.115	.026	365.231	.064	.167
	Short Duration	TD	.188	.031	365.231	.126	.249
		iASD	.154	.022	365.231	.110	.197
		PMS	.124	.026	365.231	.072	.175
Band 5	Long Duration	TD	.124	.031	365.231	.063	.186
		iASD	.096	.022	365.231	.052	.139
		PMS	.109	.026	365.231	.057	.161
	Short Duration	TD	.099	.031	365.231	.037	.160
		iASD	.090	.022	365.231	.047	.134
		PMS	.117	.026	365.231	.066	.169
Band 6	Long Duration	TD	.133	.031	365.231	.072	.195
		iASD	.105	.022	365.231	.062	.149
		PMS	.091	.026	365.231	.039	.143
	Short Duration	TD	.100	.031	365.231	.039	.162
		iASD	.095	.022	365.231	.051	.138

	PMS	.110	.026	365.231	.058	.162

a. Dependent variable: MSC.

Table 7. Multilevel Linear Models for Latency (n = 53)

	Regression coefficients (estimates of fixed effects)					
Effect	Model 1 (null)	Model 2	Model 3	Model 4	Model 5	Model 6
Intercept	140.89 (3.18)***	141.06 (4.49)***	264.591(2.69)***	263.75 (3.52)***	266.08 (3.80)***	261.65 (4.99) ***
Main effects						
Stimulus Condition						
Long	—	-.34 (6.35)	-.34 (2.03)	1.34 (4.98)	1.34 (4.96)	
Condition						1.34 (4.92)
Short	—	0[a]	0[a]	0[a]	0[a]	0[a]
Condition						
Peak-to-trough deflection						
P60	—	—	-213.03 (3.52)***	-211.85 (4.98)***	-211.85 (4.96)***	-211.14 (7.05)***
N75	—	—	-195.19 (3.52)***	-195.13 (4.98)***	-195.13 (4.96)***	-194.30 (7.05)***
P100	—	—	-164.16 (3.52)***	-163.92 (4.98)***	-163.92 (4.96)***	-158.47 (7.05)***
N135			-111.10 (3.52)***	-109.15 (4.98)***	-109.15 (4.96)***	-102.02 (7.05)***
P200	—	—	-57.73 (3.52)***	-56.13 (4.98)***	-56.13 (4.96)***	-43.73 (7.05)***
N250	—	—	0[a]	0[a]	0[a]	0[a]
Two-way interactions						
Stimulus Condition x Peak-to-trough deflection						
Long Condition x P60	—	—	—	-2.36 (7.04)	-2.36 (7.01)	-2.36 (6.95)
Long Condition x N75	—	—	—	-.11 (7.04)	-.11 (7.01)	-.11 (6.95)
Long Condition x P100	—	—	—	-.47 (7.04)	-.47 (7.01)	-.47 (6.95)
Long Condition x N135	—	—	—	-3.90 (7.04)	-3.91 (7.01)	-3.91 (6.95)

Long Condition x P200	—	—	—	-3.19 (7.04)	-3.19 (7.01)	-3.19 (6.95)
Long Condition x N250	—	—	—	0[a]	0[a]	0[a]
Short Condition x P60	—	—	—	0[a]	0[a]	0[a]
Short Condition x N75	—	—	—	0[a]	0[a]	0[a]
Short Condition x P100	—	—	—	0[a]	0[a]	0[a]
Short Condition x N135	—	—	—	0[a]	0[a]	0[a]
Short Condition x P200	—	—	—	0[a]	0[a]	0[a]
Short Condition x N250	—	—	—	0[a]	0[a]	0[a]
Main effects						
Diagnosis						
TD	—	—	—	—	-5.65 (2.78)*	-.53 (6.75)
iASD	—	—	—	—	-2.30 (2.34)	4.91 (5.67)
PMS	—	—	—	—	0[a]	0[a]
Two-way interactions						
Diagnosis x Peak-to-trough deflection						
P60 x TD	—	—	—	—	—	1.53 (9.54)
P60 x iASD	—	—	—	—	—	-2.32 (8.02)
P60 x PMS	—	—	—	—	—	0[a]
N75 x TD	—	—	—	—	—	1.14 (9.54)
N75 x iASD	—	—	—	—	—	-2.42 (8.02)
N75 x PMS	—	—	—	—	—	0[a]
P100 x TD	—	—	—	—	—	-7.04 (9.54)
P100 x iASD	—	—	—	—	—	-8.52 (8.02)
P100x PMS	—	—	—	—	—	0[a]
N135 x TD	—	—	—	—	—	-4.86 (9.54)

N135 x iASD	—	—	—	—	—	-13.32 (8.02)
N135 x PMS	—	—	—	—	—	0[a]
P200 x TD	—	—	—	—	—	-21.47 (9.54)*
P200 x iASD	—	—	—	—	—	-16.66 (8.02)
P200 x PMS	—	—	—	—	—	0[a]
N250 x TD						0[a]
N250 x iASD						0[a]
N250 x PMS						0[a]
Variance components (random effects)						
Model Summary						
-2LL[b]	7380.172	7380.1634	5930.868	5930.2813	5926.1615	5914.5625
Estimated parameters						

Note. Standard errors for parameter estimates are listed in parentheses.

[a]The parameter is set to zero because it is redundant, cross-level interactions with redundant parameters are excluded from the table.

[b]-2LL; -2 log-likelihood is a measure of how well the model fits the data. Smaller numbers reflect a better fit.

* $p < .05$. ** $p < .01$. *** $p < .001$.

Table 8. Peak-to-trough deflection x Stimulus Condition x Diagnosis

Peak-to-trough deflection			*M*	*SE*	*df*	95% Confidence Interval Lower Bound	95% Confidence Interval Upper Bound
P60	Long Condition	TD	51.250	7.284	304.782	36.917	65.583
		iASD	52.792	5.150	304.782	42.657	62.927
		PMS	47.941	6.120	304.782	35.899	59.983
	Short Condition	TD	50.750	7.284	304.782	36.417	65.083
		iASD	52.375	5.150	304.782	42.240	62.510
		PMS	52.059	6.120	304.782	40.017	64.101
N75	Long Condition	TD	68.667	7.284	304.782	54.334	83.000
		iASD	70.792	5.150	304.782	60.657	80.927
		PMS	69.353	6.120	304.782	57.311	81.395
	Short Condition	TD	68.500	7.284	304.782	54.167	82.833
		iASD	70.125	5.150	304.782	59.990	80.260
		PMS	66.588	6.120	304.782	54.546	78.630
P100	Long Condition	TD	97.083	7.284	304.782	82.750	111.416
		iASD	101.125	5.150	304.782	90.990	111.260
		PMS	102.647	6.120	304.782	90.605	114.689
	Short Condition	TD	95.000	7.284	304.782	80.667	109.333
		iASD	98.875	5.150	304.782	88.740	109.010
		PMS	104.588	6.120	304.782	92.546	116.630
N135	Long Condition	TD	155.417	7.284	304.782	141.084	169.750
		iASD	150.042	5.150	304.782	139.907	160.177
		PMS	152.471	6.120	304.782	140.429	164.513
	Short Condition	TD	150.500	7.284	304.782	136.167	164.833
		iASD	149.833	5.150	304.782	139.698	159.968
		PMS	164.235	6.120	304.782	152.193	176.277
P200	Long Condition	TD	196.333	7.284	304.782	182.000	210.666
		iASD	205.000	5.150	304.782	194.865	215.135
		PMS	213.529	6.120	304.782	201.487	225.571
	Short Condition	TD	193.667	7.284	304.782	179.334	208.000
		iASD	205.500	5.150	304.782	195.365	215.635
		PMS	220.471	6.120	304.782	208.429	232.513
N250	Long Condition	TD	266.250	7.284	304.782	251.917	280.583
		iASD	267.375	5.150	304.782	257.240	277.510
		PMS	261.059	6.120	304.782	249.017	273.101
	Short Condition	TD	257.333	7.284	304.782	243.000	271.666
		iASD	267.083	5.150	304.782	256.948	277.218

PMS	263.588	6.120	304.782	251.546	275.630

Note: Dependent variable: latency.

Table 9. Multilevel Linear Models for Ratio of Amplitude(n = 53)

	Regression coefficients (estimates of fixed effects)				
Effect	Model 1 (null)	Model 2	Model 3	Model 4	Model 5
Intercept	.87(.04)***	.93(.07)***	.92(.09)***	1.17(.12)***	1.32(.15)***
Main effects					
Peak-to-trough deflection					
P60-N75	—	.08(.09)	.08(.09)	.01(.15)	.01(.15)
N75-P100	—	-.10(.09)	-.10(.09)	-.52(.15)**	-.52(.15)**
P100-N135	—	-.09(.09)	-.09(.09)	-.57(.15)***	-.57(.15)***
N135-P200	—	-.16(.09)	-.16(.09)	-.46(.15)**	-.46(.15)**
P200-N250	—	0[a]	0[a]	0[a]	0[a]
Diagnosis					
TD	—	—	.11(.11)	-.28(.19)	-.43(.20)*
iASD	—	—	-.04(.09)	-.41(.16)**	-.56(.18)**
PMS	—	—	0[a]	0[a]	0[a]
Two-way interactions					
Diagnosis x Peak-to-trough deflection					
P60-N75 x TD	—	—	—	.08(.24)	.08(.24)
P60-N75 x iASD	—	—	—	.12(.20)	.12(.20)
P60-N75 x PMS	—	—	—	0[a]	0[a]
N75-P100 x TD	—	—	—	.63(.24)**	.63(.24)**
N75-P100 x iASD	—	—	—	.61(.20)**	.61(.20)**
N75-P100 x PMS	—	—	—	0[a]	0[a]
P100-N135 x TD	—	—	—	.74(.24)**	.74(.24)**
P100-N135 x iASD	—	—	—	.68(.20)*	.68(.20)*
P100-N135 x PMS	—	—	—	0[a]	0[a]
N135-P200 x TD	—	—	—	.47(.24)*	.47(.24)*
N135-P200 x iASD	—	—	—	.43(.20)*	.43(.20)*
N135-P200 x PMS	—	—	—	0[a]	0[a]

P200-N250 x TD	—	—	—	0[a]	0[a]
P200-N250 x iASD	—	—	—	0[a]	0[a]
P200-N250 x PMS	—	—	—	0[a]	0[a]
Main effects					
Deletion					
None (TD)	—	—	—	—	0[a]
None (iASD)	—	—	—	—	0[a]
Point	—	—	—	—	-.38(.18)*
Mutation					
Small Deletion	—	—	—	—	-.14(.16)
Large Deletion	—	—	—	—	0[a]
Variance components (random effects)					
Model Summary					
-2LL[b]	391.919	383.576	381.516	359.948	355.728
Estimated parameters	3	7	9	17	19

Note. Standard errors for parameter estimates are listed in parentheses.

[a]The parameter is set to zero because it is redundant, cross-level interactions with redundant parameters are excluded from the table.

[b]-2LL; -2 log-likelihood is a measure of how well the model fits the data. Smaller numbers reflect a better fit.

* $p < .05$. ** $p < .01$. *** $p < .001$.

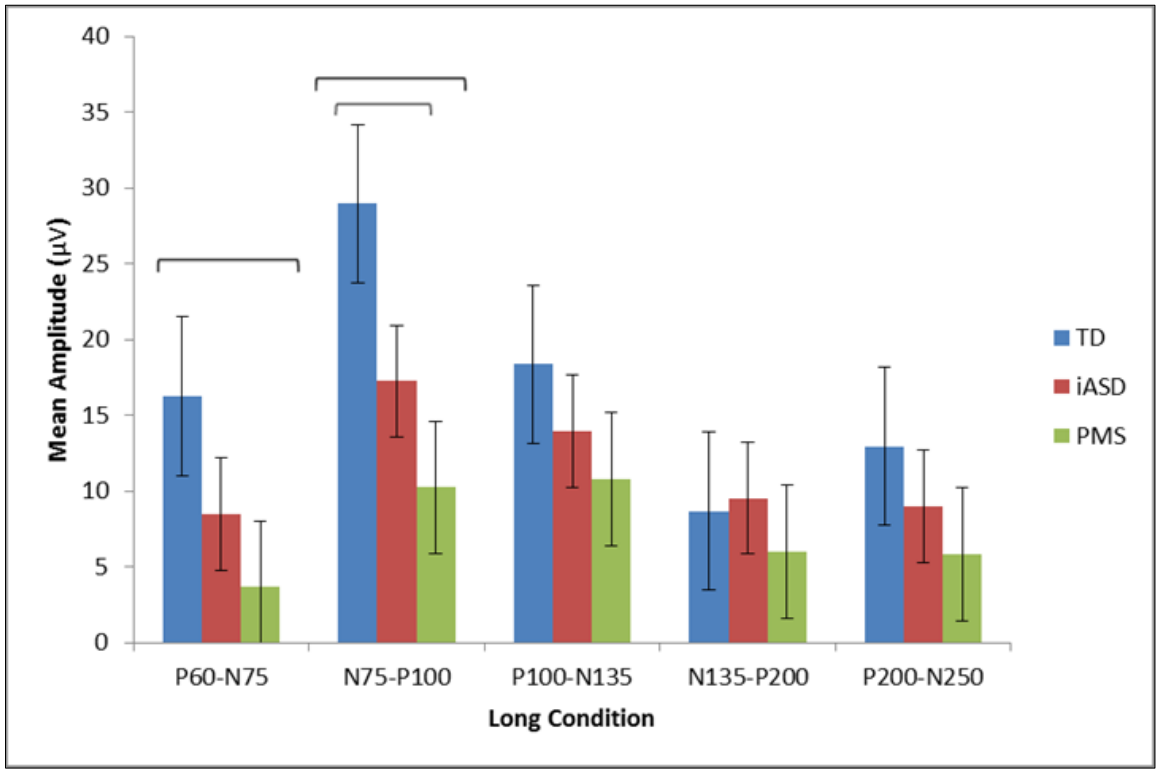

Figure 1. Mean amplitude by group for the long condition contrast-reversing checkerboard (60-s epochs). Significance brackets indicate p-values < .05. Error bars are 95% confidence intervals.

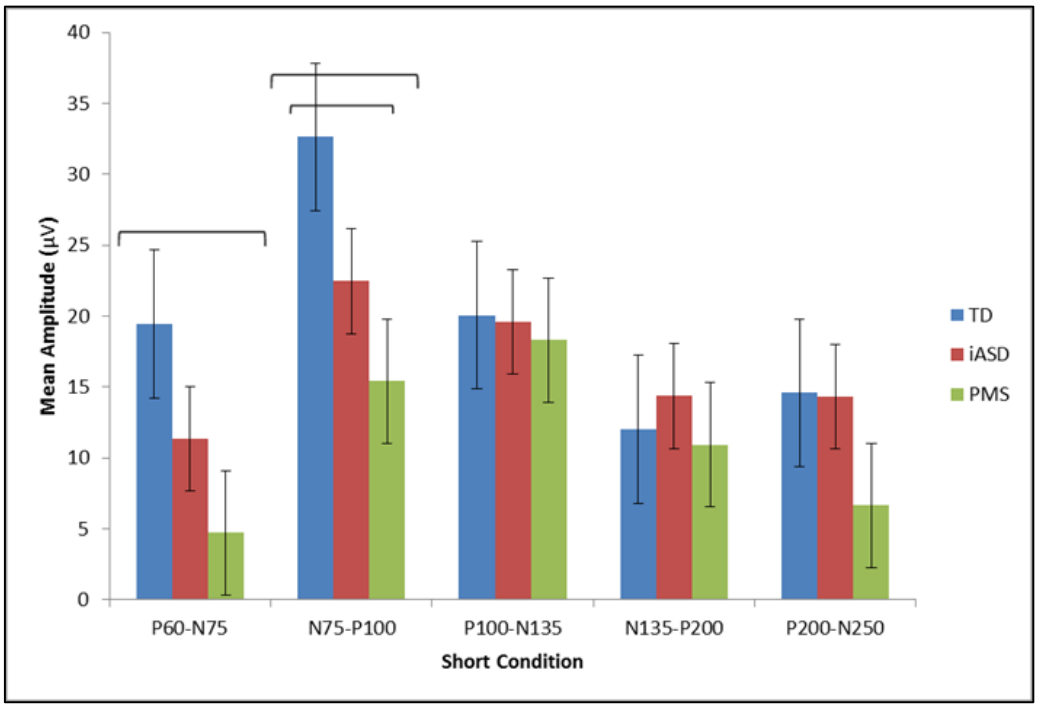

Figure 2. Mean amplitude by group for the short condition contrast-reversing checkerboard (ten trials of 3-s epochs). Significance brackets indicate p-values < .05. Error bars 95% confidence intervals.

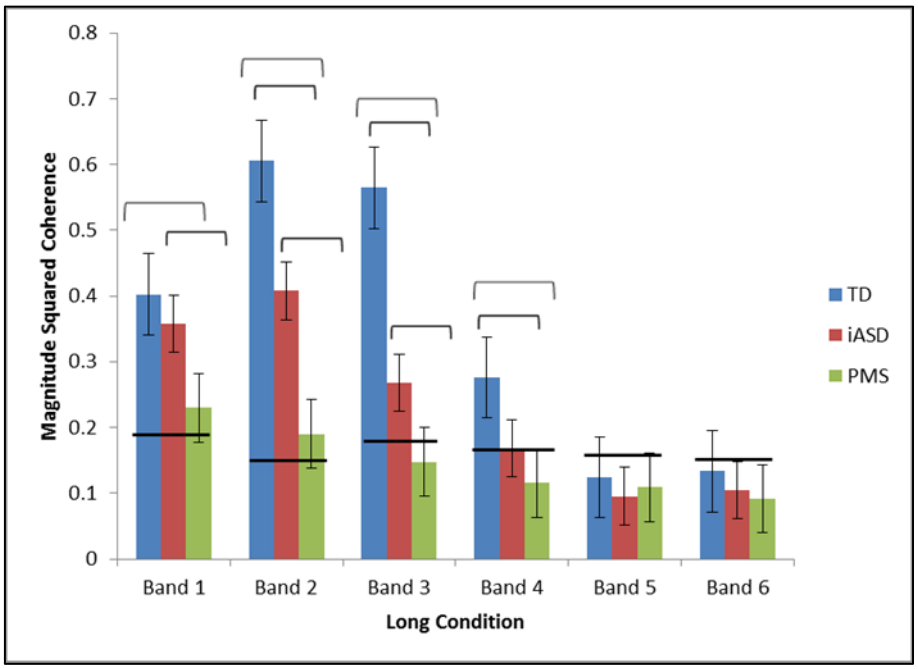

Figure 3. Mean magnitude squared coherence (MSC) is plotted for each band in the long condition (60-s contrast-reversing checkerboard) by group. MSC is the estimate of *signal power/signal noise+power*. Error bars represent the 95% confidence intervals. Solid horizontal bars indicate the critical value for MSC. Significant differences of MSC per band between groups are indicated by the brackets, *p*-values < .05.

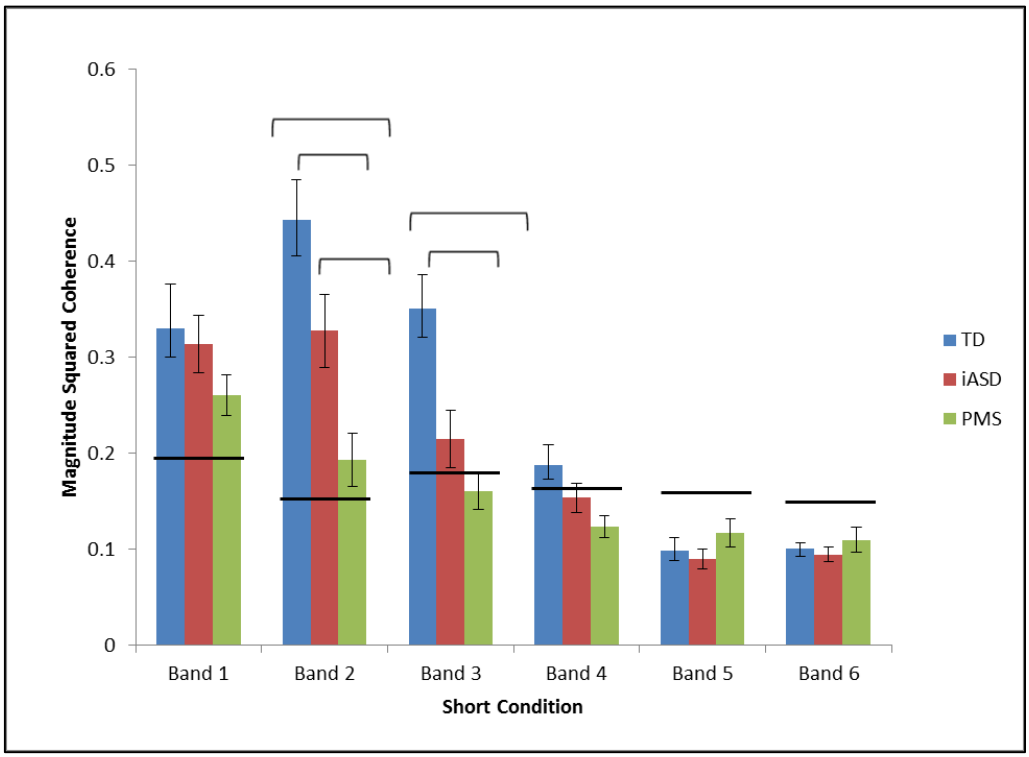

Figure 4. Mean magnitude squared coherence (MSC) is plotted for each band in the short condition contrast-reversing checkerboard (ten trials of 3-s epochs) by group. MSC is the *signal power/signal noise+power*. Error bars represent the 95% confidence interval. Solid horizontal bars indicate the critical value for MSC. Significant differences of MSC of band between groups is indicated by the brackets, *p*-values < .05.

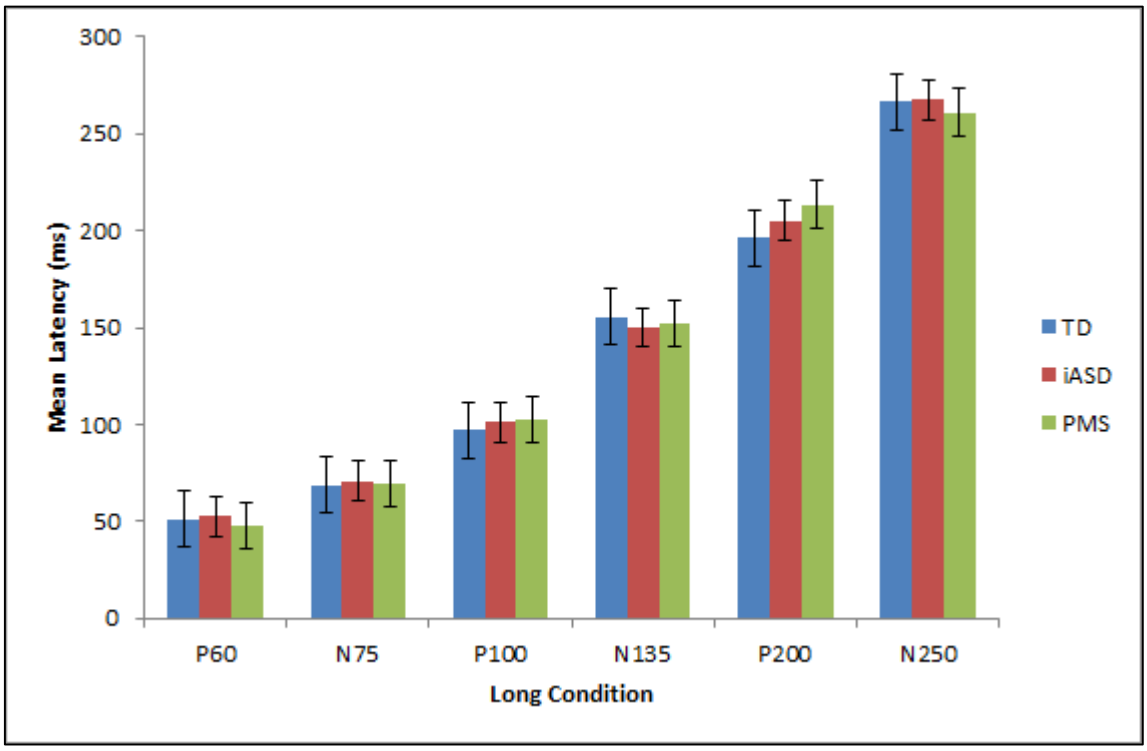

Figure 5. Latency of peak deflections in the long condition for groups. Error bars represent the 95% confidence intervals. No significant differences were found.

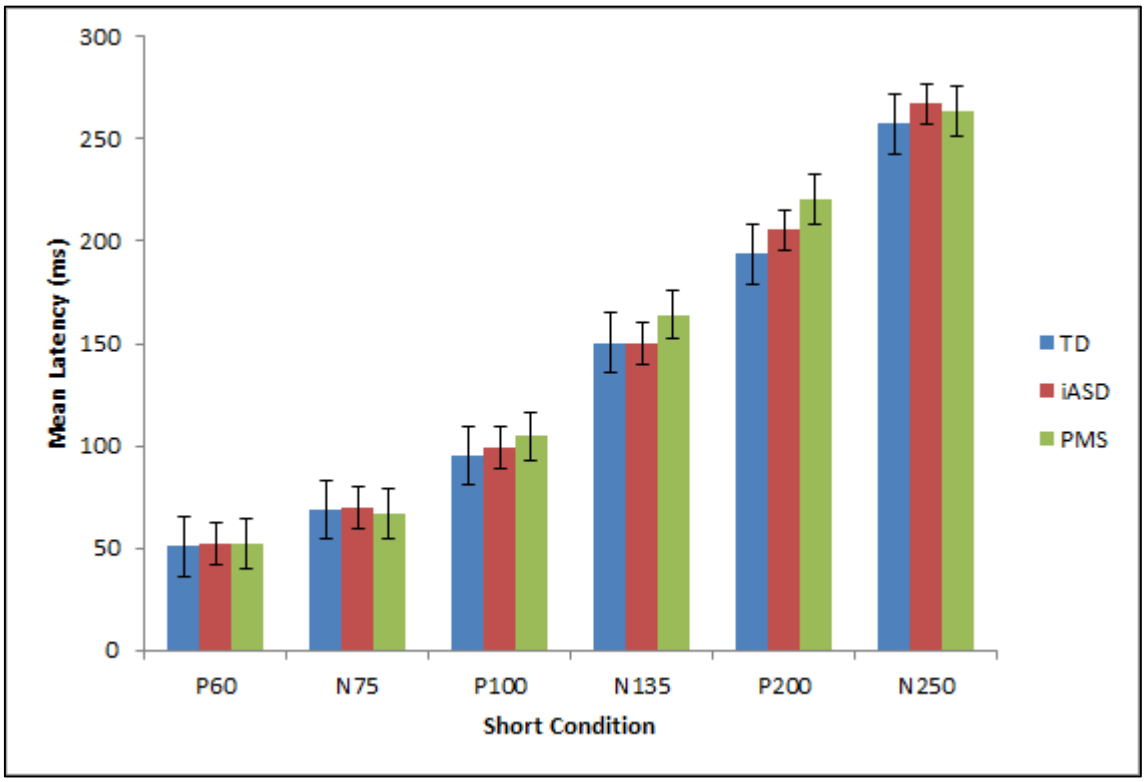

Figure 6. Latency of peak deflections in the short condition for groups. Error bars represent the 95% confidence interval.

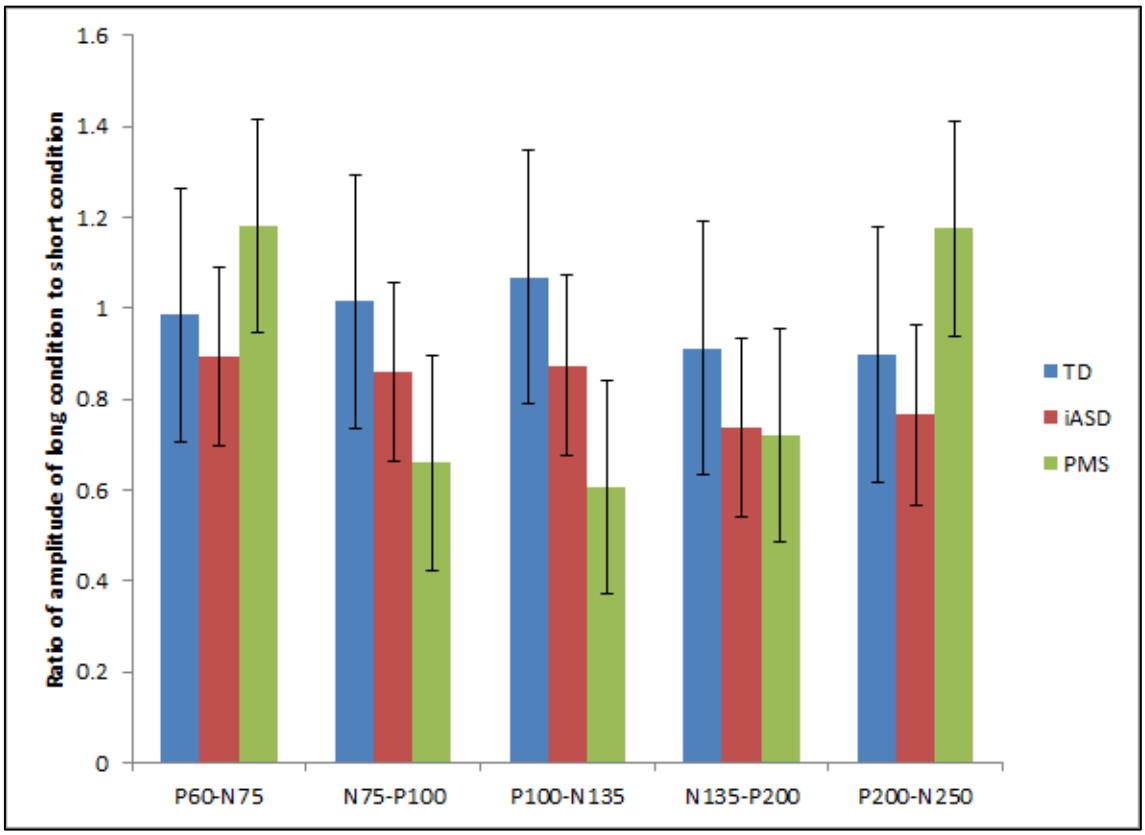

Figure 7. Ratio of peak-to trough amplitude of long to short conditions by group. Error bars represent the 95% confidence interval.

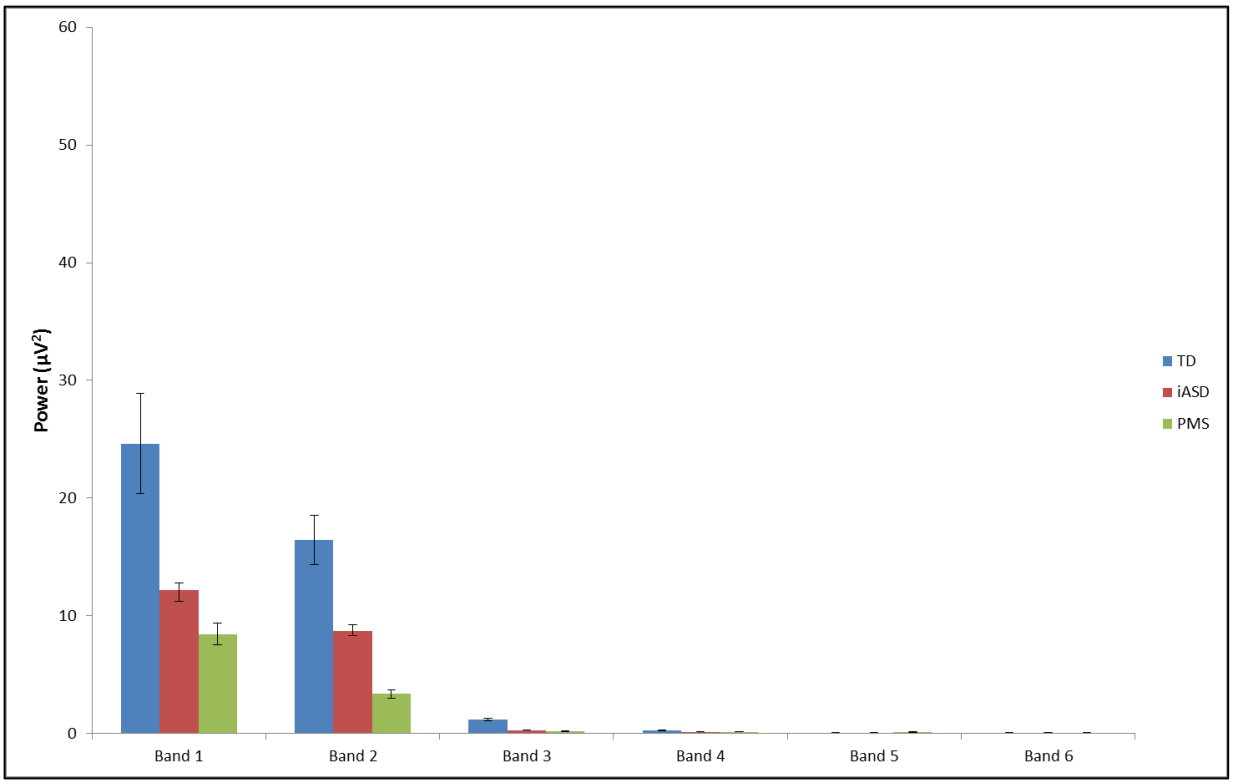

Figure 8. Power at frequencies in Bands 1-6 in the long condition (60-s contrast-reversing checkerboard). Error bars represent 95% confidence intervals.

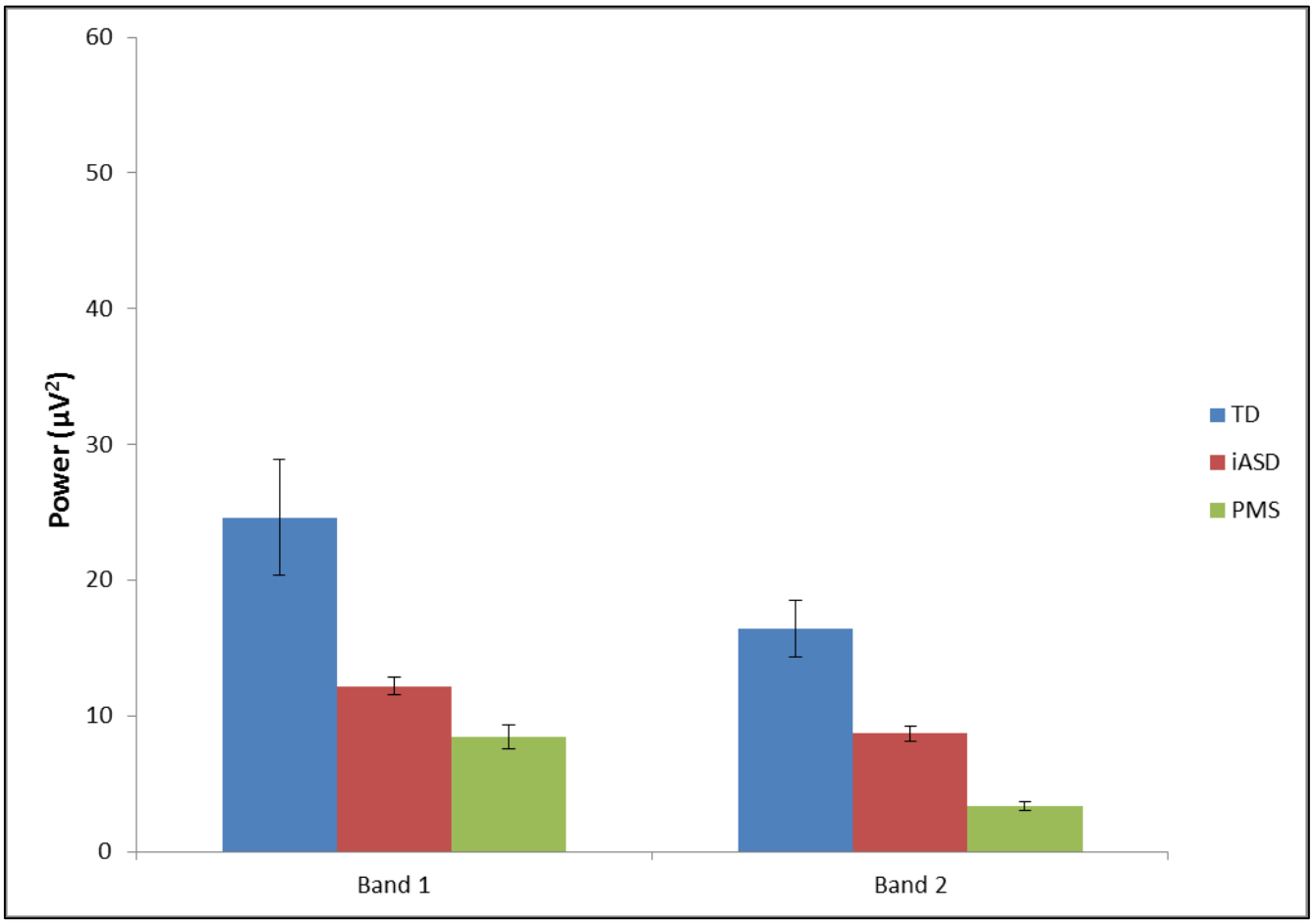

Figure 9. Power at frequencies in Band 1 and Band 2 in the long condition (60-s contrast-reversing checkerboard). Error bars represent 95% confidence intervals.

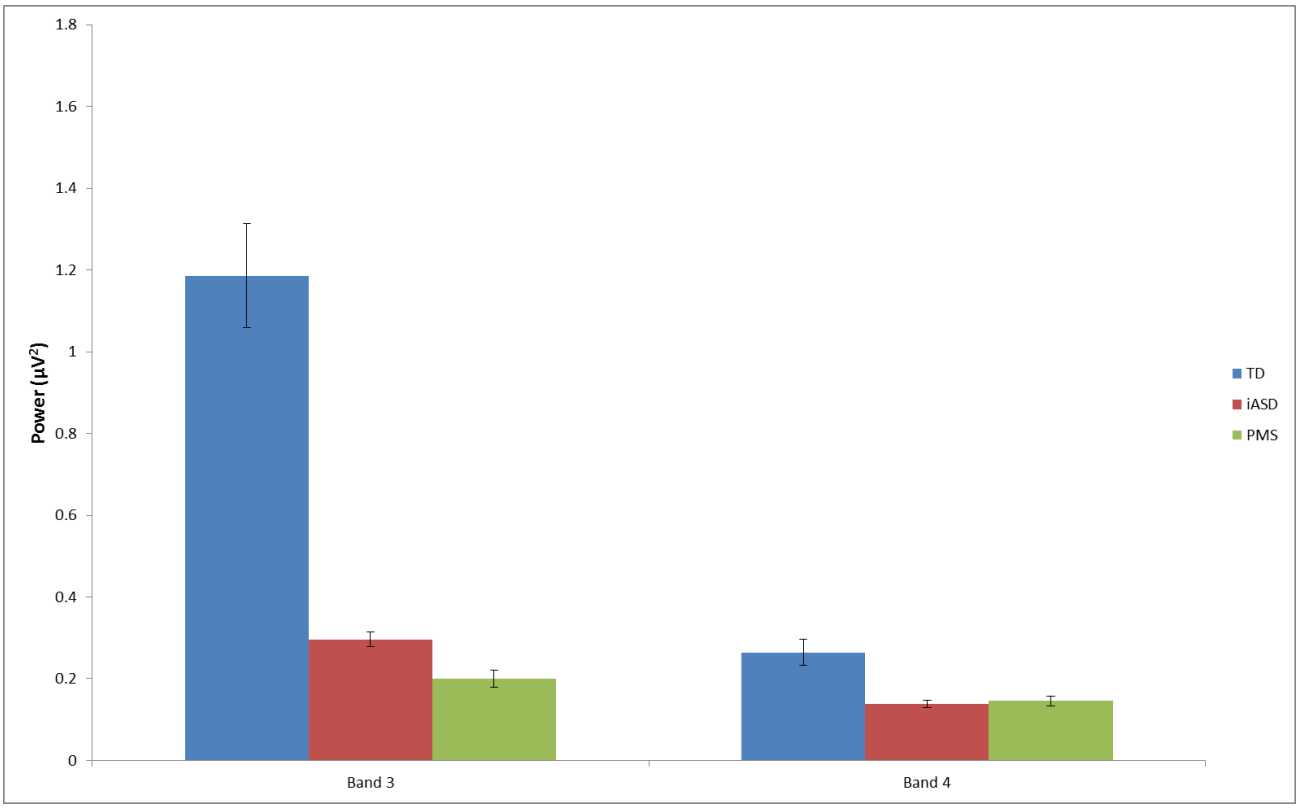

Figure 10. Power at frequencies in Bands 3 and 4 in the long condition (60-s contrast-reversing checkerboard). Error bars represent 95% confidence intervals.

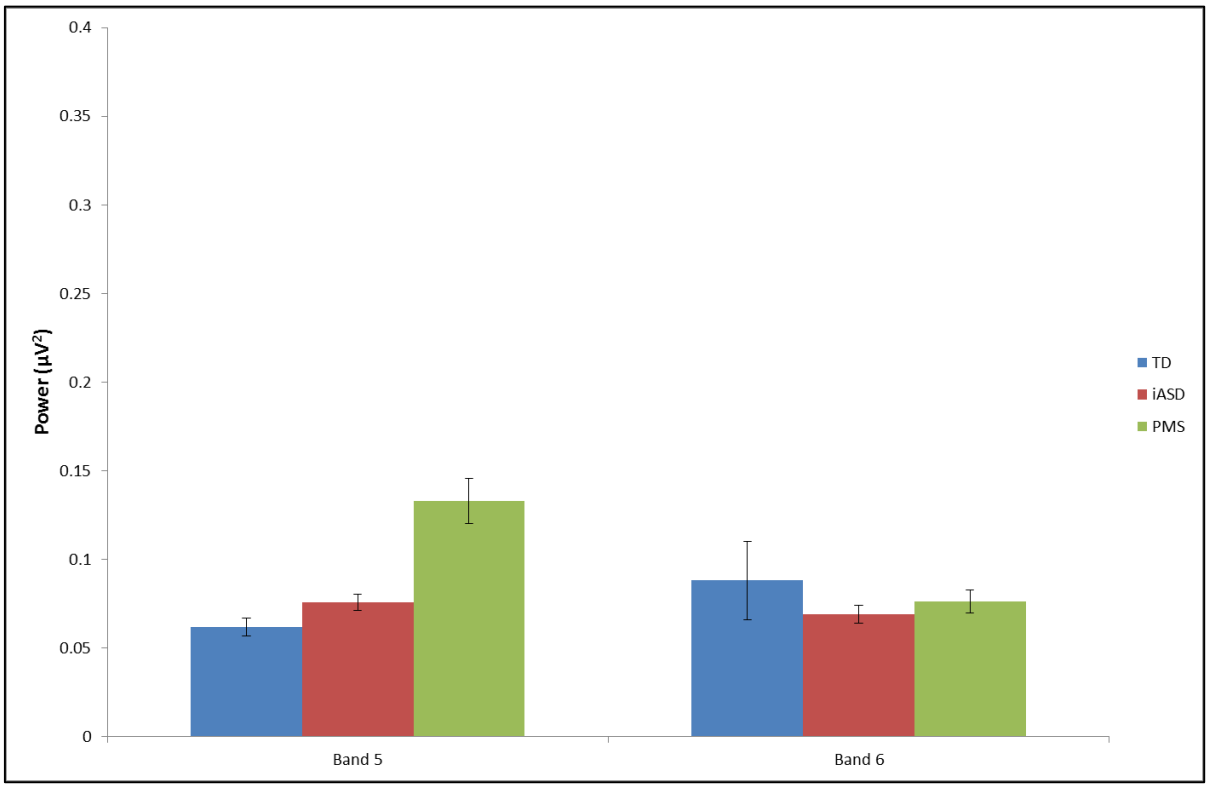

Figure 11. Power at frequencies in Bands 5 and 6 in the long condition (60-s contrast-reversing checkerboard). Error bars represent 95% confidence intervals.

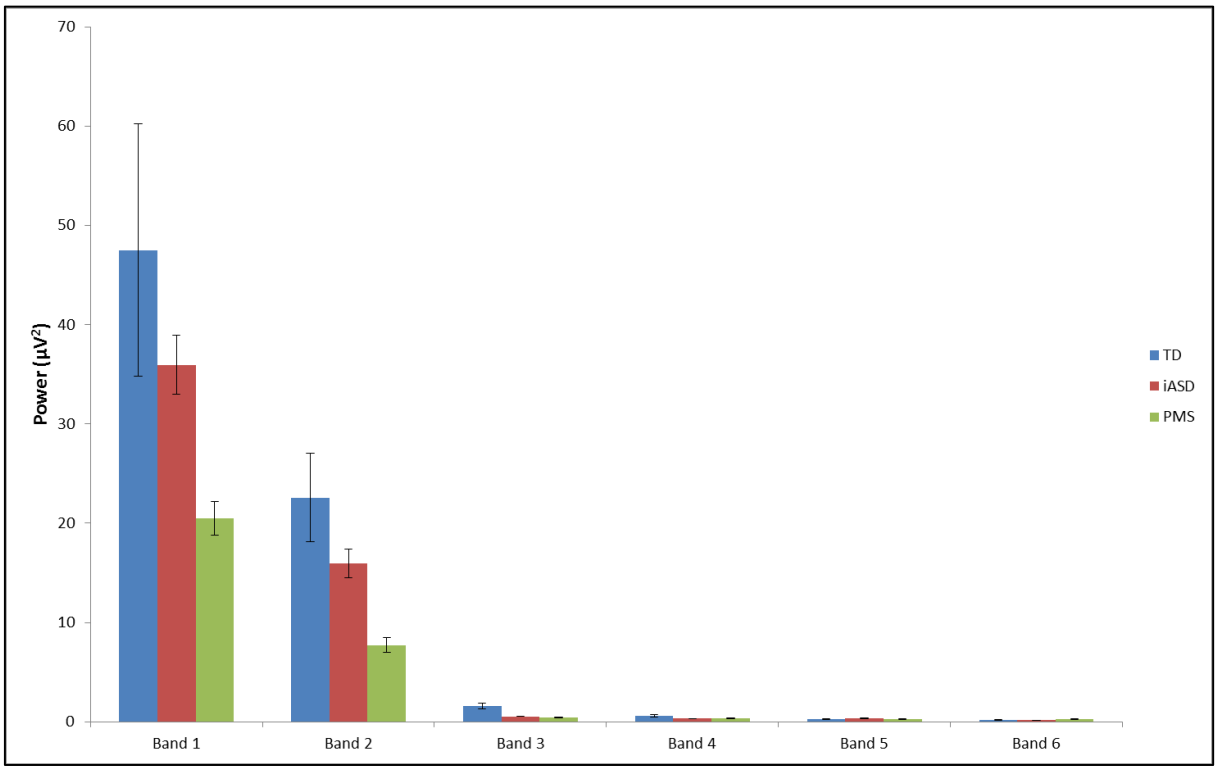

Figure 12. Power at frequencies in Bands 1-6 in the short condition contrast-reversing checkerboard (ten trials of 3-s epochs). Error bars represent 95% confidence intervals.

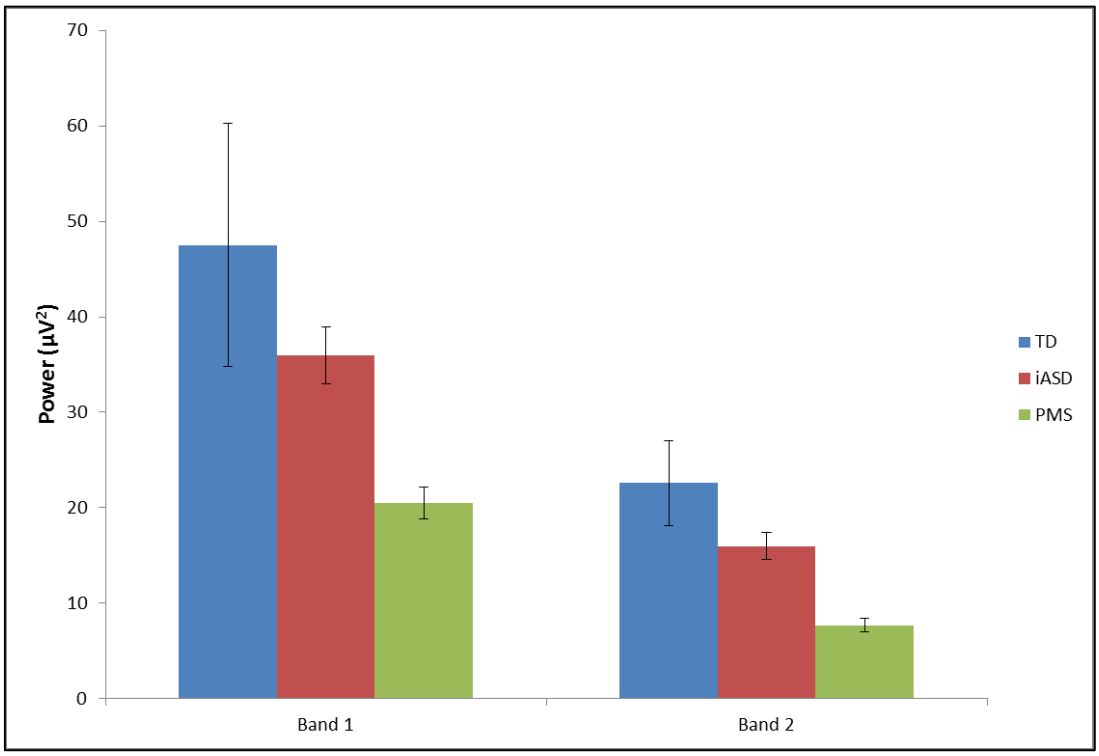

Figure 13. Power at frequencies in Bands 1 and 2 in the short condition contrast-reversing checkerboard (ten trials of 3-s epochs). Error bars represent 95% confidence intervals.

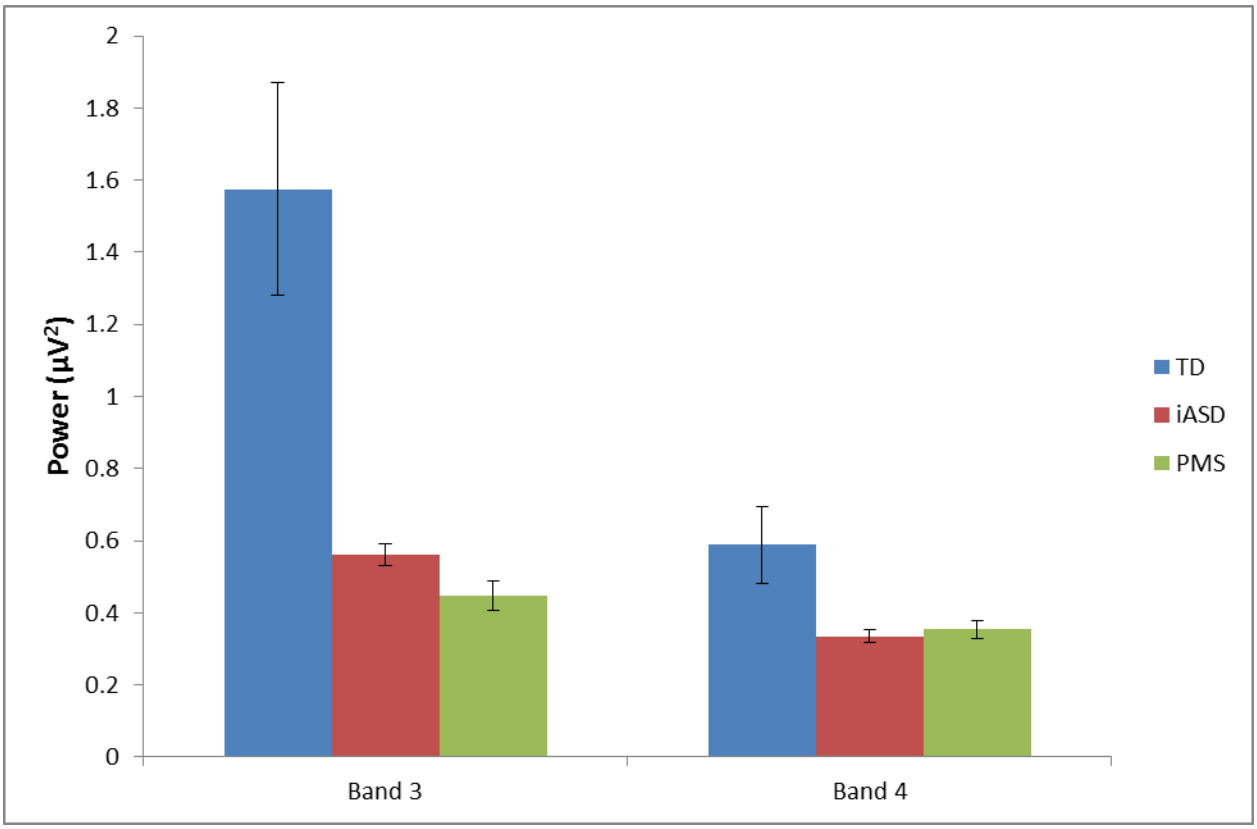

Figure 14. Power at frequencies in Bands 3 and 4 in the short condition contrast-reversing checkerboard (ten trials of 3-s epochs). Error bars represent 95% confidence intervals.

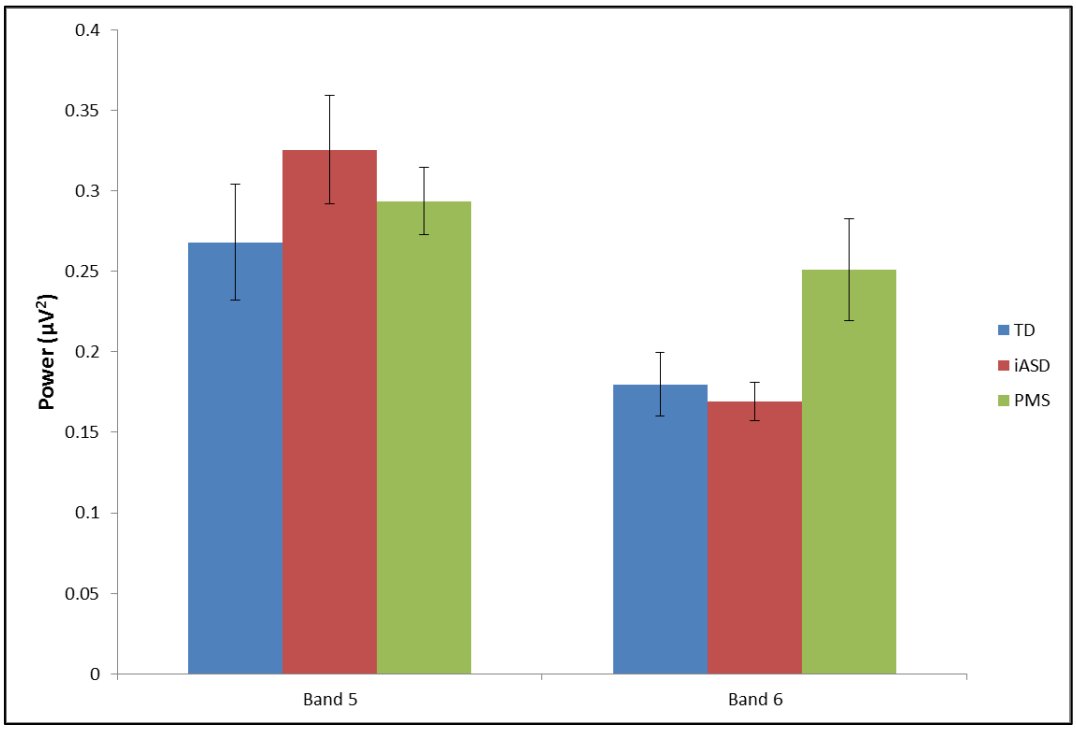

Figure 15. Power at frequencies in Bands 5 and 6 in the short condition contrast-reversing checkerboard (ten trials of 3-s epochs). Error bars represent 95% confidence intervals.

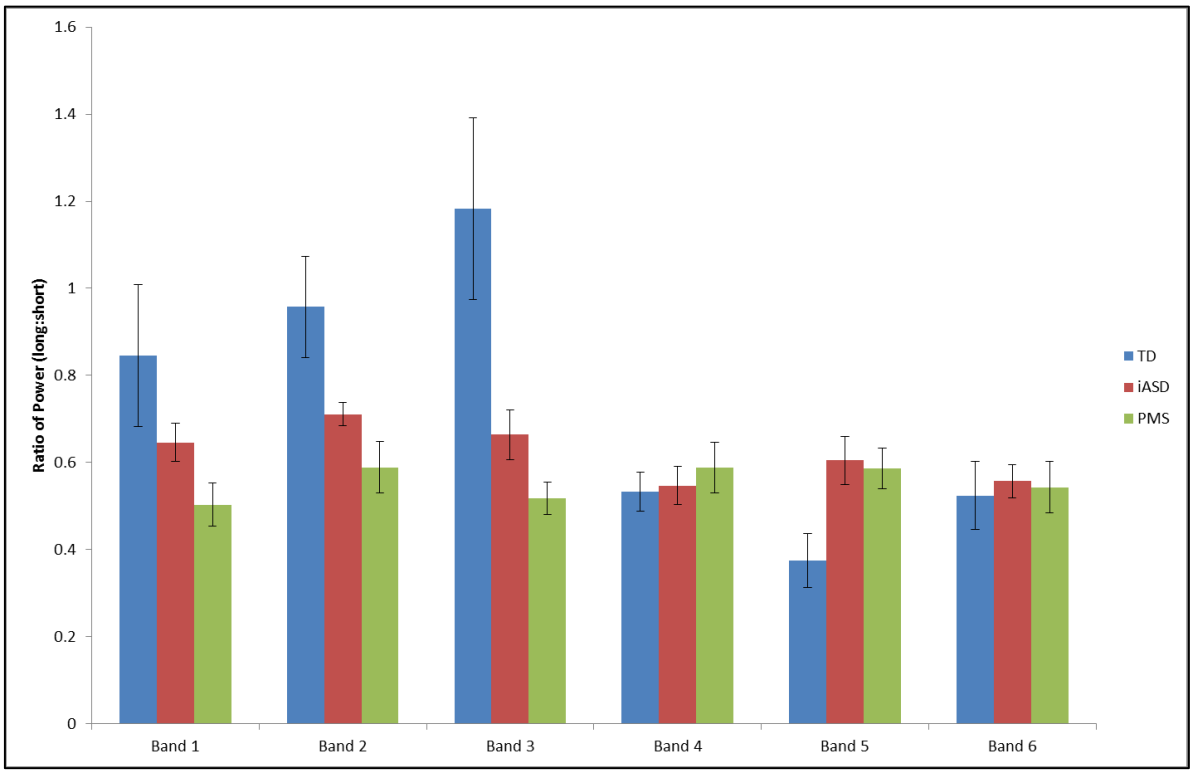

Figure 16. Ratio of power in frequency bands, from long- to short-duration conditions. Error bars represent 95% confidence intervals.